

# M<sup>3</sup>Prune: Hierarchical Communication Graph Pruning for Efficient Multi-Modal Multi-Agent Retrieval-Augmented Generation

Weizi Shao<sup>1\*</sup>, Taolin Zhang<sup>2\*</sup>, Zijie Zhou<sup>3</sup>, Chen Chen<sup>4</sup>, Chengyu Wang<sup>5†</sup>, Xiaofeng He<sup>1†</sup>

<sup>1</sup> East China Normal University, Shanghai, China <sup>2</sup> Hefei University of Technology, Hefei, China

<sup>3</sup> China University of Petroleum, Beijing, China

<sup>4</sup> Guangdong university of Finance & Economics, Guangdong, China <sup>5</sup> Alibaba Group, Hangzhou, China

51265901007@stu.ecnu.edu.cn, tlzhang@hfut.edu.cn

chengyu.wcy@alibaba-inc.com, hexf@cs.ecnu.edu.cn

## Abstract

Recent advancements in multi-modal retrieval-augmented generation (mRAG), which enhance multi-modal large language models (MLLMs) with external knowledge, have demonstrated that the collective intelligence of multiple agents can significantly outperform a single model through effective communication. Despite impressive performance, existing multi-agent systems inherently incur substantial token overhead and increased computational costs, posing challenges for large-scale deployment. To address these issues, we propose a novel **Multi-Modal Multi-agent hierarchical communication graph PRUNING** framework, termed **M<sup>3</sup>Prune**. Our framework eliminates redundant edges across different modalities, achieving an optimal balance between task performance and token overhead. Specifically, M<sup>3</sup>Prune first applies intra-modal graph sparsification to textual and visual modalities, identifying the edges most critical for solving the task. Subsequently, we construct a dynamic communication topology using these key edges for inter-modal graph sparsification. Finally, we progressively prune redundant edges to obtain a more efficient and hierarchical topology. Extensive experiments on both general and domain-specific mRAG benchmarks demonstrate that our method consistently outperforms both single-agent and robust multi-agent mRAG systems while significantly reducing token consumption.<sup>1</sup>

## 1. Introduction

While retrieval-augmented generation (RAG) has achieved significant success in the textual domain [9, 20, 56], extend-

ing it to the multi-modal realm presents substantial challenges [17]. Traditional methods typically rely on a cascaded pipeline in which a multi-modal retriever extracts relevant evidence, which is then forwarded to LLMs for answer synthesis [15, 18, 36]. This segmented approach inherently suffers from global semantic alignment gap [19, 24].

The emergence of multi-modal large language models (MLLMs) presents a transformative opportunity, as these models possess a remarkable ability to understand visual-language correlations [3, 12, 39]. This capability enables MLLMs to function not only as generators but also as integrative engines for multi-modal RAG (mRAG). By jointly processing retrieved multi-modal evidence and questions within a cohesive reasoning backbone, MLLMs can synthesize information and derive coherent conclusions from retrieved knowledge [31, 54, 58]. Nonetheless, when confronted with complex, multi-faceted multi-modal questions that demand diverse expertise or deliberative reasoning, a single agent often reaches its limitations [10, 33, 49].

Recent efforts have investigated multi-agent systems built upon MLLMs, in which multiple specialized agents collaboratively communicate through structured graph topologies to distribute reasoning workloads for complex multi-modal tasks [17, 32, 34, 51]. However, performance improvements often come at a substantial cost, notably a significant increase in computational and token overhead. Critically, we identify the root cause (Communication Redundancy), which not only induces inefficiency but also directly undermines the accuracy of the final response [17, 53]. This redundancy is especially pronounced in multi-modal settings, where the informational requirements for processing textual cues and visual patterns inherently differ. Yet, existing methods frequently employ intra-modal communication strategies across all modalities [22, 27, 44]. As shown in Fig. 1, in the “first flight date” question, the date expert agent is overwhelmed by irrele-

\* W. Shao and T. Zhang contributed equally to this work.

† Co-corresponding authors.

<sup>1</sup>Source code is provided in the supplementary material and will be released upon acceptance.

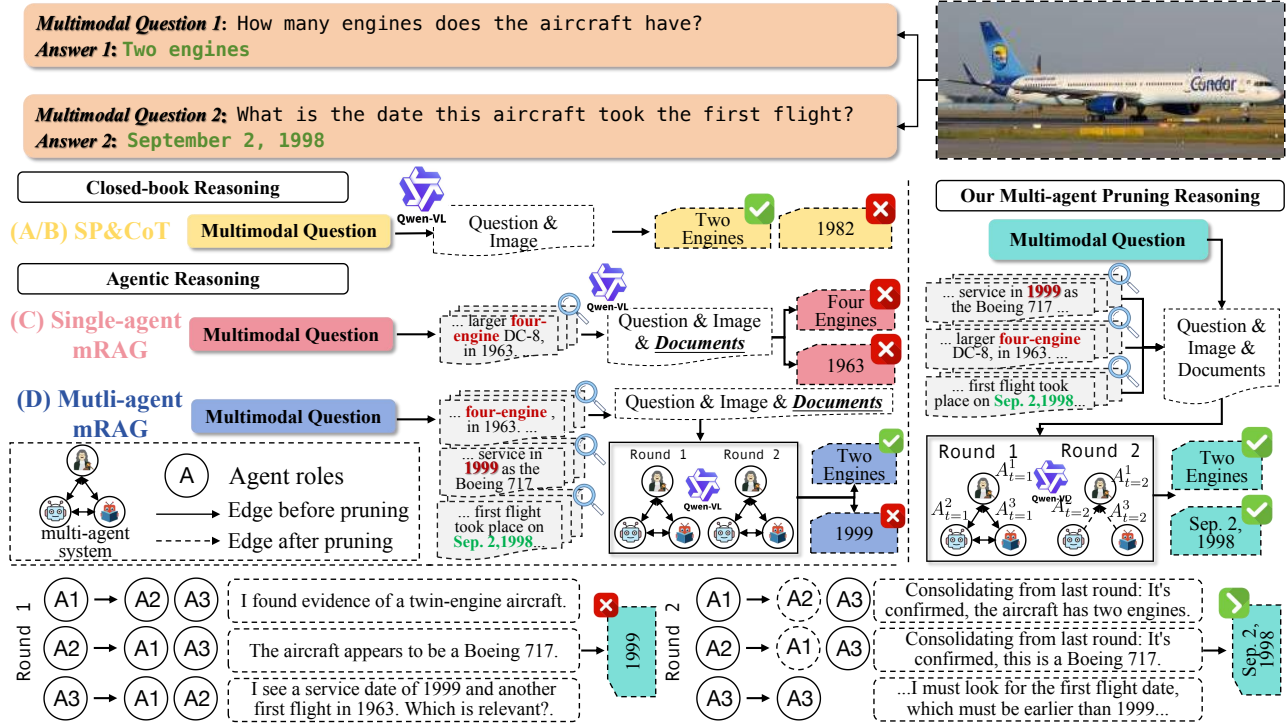


Figure 1. Comparison of our approach with existing methods. (1) Closed-book Reasoning does not consider the need for external knowledge. (2) Single-agent mRAG leverages an end-to-end MLLM solution combined with a retriever to answer all questions. (3) Multi-agent mRAG constructs a fixed communication topology to obtain collaborative answers, regardless of communication efficiency. (4) Our Multi-agent Pruning approach dynamically prunes unnecessary edge connections to enhance response consistency.

vant messages about engine counts and models. This noise prevents filtering out incorrect dates and obscures the correct evidence, leading to an erroneous answer.

We introduce **M<sup>3</sup>Prune**, a novel framework for hierarchical communication graph pruning in multi-agent mRAG systems. Two key modules of M<sup>3</sup>Prune are as follows:

**Intra-Modal Graph Sparsification:** In mRAG tasks, agents assigned different roles may hold divergent viewpoints on the same question [50, 57]. Consequently, there can be both cooperation and conflict among agents within the same modality, which may hinder mutual enhancement. To address this, we design a spatio-temporal message-passing technique that facilitates effective exchange of viewpoints within the visual and textual modalities, respectively. The significance of edge connections between agents in each modality is determined by the quality of the final response and the structure of the communication topology. For redundant edges connecting agents with low contribution within a modality, communication with other key agents is substantially reduced by sparsifying edge weights.

**Inter-Modal Graph Sparsification:** Given the diverse effects of information granularity across modalities, it is essential to comprehensively integrate key clues from multiple modalities before generating the final response [2, 7, 23, 41]. Therefore, we aggregate the roles of agents across

modalities to construct an inter-modal spatio-temporal communication topology, facilitating robust inter-modal collaboration and resolution of viewpoint conflicts. Specifically, we initialize the inter-modal communication topology based on intra-modal sparse graphs and diverse agent role correlations, integrating cross-modal text-visual and visual-text role viewpoints to learn the significance of inter-modal edges. In addition to optimizing for task performance and structural regularity, analogous to intra-modal learning, we further incorporate a modality alignment loss to ensure consistency in task understanding across different modalities during inter-modal topology sparsification. Finally, after learning edge sparsity weights within hierarchical intra- and inter-modal graphs, we progressively prune invalid edges associated with redundant agent roles across modalities.

In our experiments, we evaluate M<sup>3</sup>Prune against a range of strong baselines, including zero-shot, single-agent, and multi-agent multi-modal settings on mRAG benchmarks: Vidoseek [42], MultimodalQA [38], and ScienceQA [28], which cover general and domain-specific tasks. Results show that our approach achieves state-of-the-art performance, with an improvement of **9.4%** in accuracy while significantly reducing token consumption by **15.7%** compared to strong multi-modal multi-agent baselines.

## 2. Related Works

### 2.1. Multi-Modal Retrieval-Augmented Generation

Previous works in mRAG can be broadly categorized into two interconnected themes: (1) **Modality-Adaptive Retrieval Strategies**. A key limitation of early mRAG systems is their static retrieval approach, which often resulted in unnecessary computational overhead [11, 28, 30]. Recent works have introduced dynamic, query-aware strategies to determine whether to retrieve and which modality to retrieve from. For example, EchoSight [48] and RoRA-VLM [35] search wiki articles using visual-only information, then re-rank them according to their relevance to the combined text-visual question. (2) **Retrieval-Aware Pre-Training/Fine-Tuning**. CoRe-MMRAG [40] reconciles inconsistencies across different knowledge sources through a four-stage progressive multi-modal retrieval pipeline. LLaVA-mR<sup>2</sup>AG [55] introduces a fine-tuned adaptive retriever that derives answers using two straightforward reflection operations. Wiki-LLaVA [6] employs a hierarchical retrieval pipeline to integrate external knowledge from multi-modal documents. These methods leverage single MLLM as the backbone but overlook the substantial advantage of swarm intelligence in enhancing mRAG tasks [17].

### 2.2. Multi-Agent Systems for mRAG

The area can be categorized into several research directions: (1) **General Agentic Collaboration**. A significant paradigm shift has been the move from static retrieval and generation to agentic designs, transforming passive pipelines into active, decision-making systems [8, 26, 50]. ViDoRAG [42] introduces an iterative agent workflow that combines exploration, summarization, and reflection, providing a framework for test-time scaling in mRAG. OmniSearch [22] designs a self-adaptive planning agent for retrieval, emulating human behavior by dynamically decomposing complex multi-modal questions into sub-questions with adaptive retrieval actions. E-agent [44] proposes a plan-then-execute architecture that combines a dynamic mRAG planner with a tool executor. (2) **Evolving Collaborative Architectures**. As mRAG task complexity increases, the limitations of general multi-agent systems become apparent, prompting the development of multi-modal agent collaboration [13, 37]. HM-RAG [27] employs a hierarchy of agents, including a decomposer agent to break down multi-intent queries and a decision agent to synthesize the final answer. MuALLM [1] integrates a hybrid mRAG framework that includes iterative reasoning, goal setting, and multi-step retrieval with an adaptive vector database. While current research demonstrates significant gains in handling complex mRAG tasks through multi-agent collaboration, redundant and inefficient agent roles can reduce overall efficiency [17, 53]. Hence, we propose a hierar-

chical multi-modal multi-agent edge pruning framework to maintain performance while reducing the token overhead.

## 3. Basic Notations and Task Definition

### 3.1. Basic Notations

Our hierarchical framework consists of intra- and inter-modal graph pruning modules.<sup>2</sup> The intra-modal module comprises a textual graph,  $\mathcal{G}_{txt}^{intra} = (\mathcal{V}_{txt}, \mathcal{E}_{txt}^T, \mathcal{E}_{txt}^S, \mathcal{S}_{txt})$ , and a visual graph,  $\mathcal{G}_{vis}^{intra} = (\mathcal{V}_{vis}, \mathcal{E}_{vis}^T, \mathcal{E}_{vis}^S, \mathcal{S}_{vis})$ , where  $\mathcal{V}_{txt} = \{v_1^{txt}, v_2^{txt}, \dots, v_{|\mathcal{V}_{txt}|}^{txt}\}$  and  $\mathcal{V}_{vis} = \{v_1^{vis}, v_2^{vis}, \dots, v_{|\mathcal{V}_{vis}|}^{vis}\}$  denote the sets of textual and visual agent nodes, respectively. Each agent node is initialized with either a textual or a visual role.  $\mathcal{E}_{txt}^T$  and  $\mathcal{E}_{txt}^S$  denote the textual temporal and spatial edge sets, respectively,<sup>3</sup> with  $\mathcal{S}_{txt}^{(t)} = \{s_1^{txt,(t)}, s_2^{txt,(t)}, \dots, s_{|\mathcal{S}_{txt}|}^{txt,(t)}\}$  representing the memory of each textual agent at round  $t$ . Correspondingly,  $\mathcal{E}_{vis}^T$  and  $\mathcal{E}_{vis}^S$  denote the visual temporal and spatial edge sets, with  $\mathcal{S}_{vis}^{(t)} = \{s_1^{vis,(t)}, s_2^{vis,(t)}, \dots, s_{|\mathcal{S}_{vis}|}^{vis,(t)}\}$  representing the memory of each visual agent. The memory transition of each agent between two rounds is formulated as:

$$s_i^{m,(t+1)} = f_{tr} \left( s_i^{m,(t)}, \mathbf{q}, \mathbf{c}, I_{\mathcal{T}}^{m,(t+1)}, I_{\mathcal{S}}^{m,(t+1)} \right) \quad (1)$$

where  $f_{tr}$  denotes that we use the specific MLLM-based agents to aggregate information to update the memory in the current round. Here,  $m \in \{\text{txt}, \text{vis}\}$  indexes the two modalities, while  $\mathbf{q}$  and  $\mathbf{c}$  represent the task question and the retrieved contexts, respectively.  $I_{\mathcal{T}}^{m,(t+1)}$  and  $I_{\mathcal{S}}^{m,(t+1)}$  denote the information aggregated from the temporal and spatial neighbors for modality  $m$  at round  $(t+1)$ .

For the inter-modal part, all textual and visual agent nodes are incorporated into an independent inter-modal graph,  $\mathcal{G}^{inter} = (\mathcal{V}, \mathcal{E}^T, \mathcal{E}^S, \mathcal{S})$ . The node set is defined as  $\mathcal{V} = \mathcal{V}_{txt} \cup \mathcal{V}_{vis}$ . The temporal edge set  $\mathcal{E}^T$  integrates both intra-modal and inter-modal connections, defined as  $\mathcal{E}^T = \mathcal{E}_{txt}^T \cup \mathcal{E}_{vis}^T \cup \mathcal{E}_{vis \rightarrow txt}^T \cup \mathcal{E}_{txt \rightarrow vis}^T$ . Similarly, the spatial edge set is  $\mathcal{E}^S = \mathcal{E}_{txt}^S \cup \mathcal{E}_{vis}^S \cup \mathcal{E}_{vis \rightarrow txt}^S \cup \mathcal{E}_{txt \rightarrow vis}^S$ . Intra-modal edges in the temporal and spatial sets are inherited from the intra-modal graphs, while inter-modal edges are initialized as fully connected. Finally, the joint agent memory is given by  $\mathcal{S} = \mathcal{S}_{txt} \cup \mathcal{S}_{vis}$ . The memory update mechanism is similar to that in the intra-modal graph (see Eq. 1), except that  $I_{\mathcal{T}}^{(t+1)}$  and  $I_{\mathcal{S}}^{(t+1)}$  may originate from inter-modal temporal and spatial connections.

### 3.2. Task Definition

Given a question  $\mathbf{q}$  and retrieved contexts  $\mathbf{c}$ , each agent in an intra-modal graph is restricted to receiving information only

<sup>2</sup>All mathematical notations and agent prompt descriptions are summarized in Appendix 7.

<sup>3</sup>Each agent is fully connected to all other agents except itself for spatial edges, and connected to all agents including itself for temporal edges.

from edges within the same modality, whereas in an inter-modal graph, agents may also receive output information from inter-modal agents.<sup>4</sup> For each agent, its output viewpoint at round  $t$  is defined as:  $\mathcal{O}_i^{(t)} = f_\theta(\mathbf{q}, \mathbf{c}, I_{\mathcal{T}}^{(t)}, I_{\mathcal{S}}^{(t)})$  where  $f_\theta$  denotes the MLLM-generated response based on the task question, retrieved context, and both temporal and spatial information for the agent. Each agent outputs sequentially according to the order defined by the DAG in each round. After multiple rounds of multi-agent interaction, we additionally employ a summary agent to produce the final answer:  $\mathcal{O}_s^{(T)} = f_s(\mathbf{q}, \mathbf{c}, I_{\mathcal{T}}^{(T)}, I_{\mathcal{S}}^{(T)})$  where  $T$  is the total number of rounds,  $f_s$  denotes the summary agent, and  $\mathcal{O}_s^{(T)}$  is the final answer. However, a fixed communication topology inevitably yields redundant information, necessitating the pruning of superfluous edges [22, 44]. Consequently, we formally define the notion of communication redundancy to guide the pruning process:

**Definition 1 (Communication Redundancy).** Given a multi-modal multi-agent communication graph  $\mathcal{G}^{\text{intra/inter}} = (\mathcal{V}, \mathcal{E}^{\mathcal{T}}, \mathcal{E}^{\mathcal{S}}, \mathcal{S})$ , an edge  $e$  is considered redundant if it meets the following condition:

$$\begin{aligned} \forall e \in \mathcal{E}^{\mathcal{S}} \cup \mathcal{E}^{\mathcal{T}}, \quad \mathcal{G}^{\text{sub}} = (\mathcal{V}, \{\mathcal{E}^{\mathcal{S}} \cup \mathcal{E}^{\mathcal{T}}\} \setminus \{e\}) \subseteq \mathcal{G}, \\ \text{s.t. } \phi(\mathcal{G}^{\text{sub}}) \geq \phi(\mathcal{G}) \end{aligned} \quad (2)$$

where  $\phi(\cdot)$  is a utility function that evaluates the task performance. In particular, the goal of inter-modal edge pruning is constructing  $\mathcal{G}^{\text{sub}}$  by removing redundant edges while maintaining task performance [53], which is further enforced by modality semantic alignment [2]:

$$\begin{aligned} \text{argmax}_{\mathcal{E}_p} |\mathcal{G} \setminus \mathcal{G}^{\text{sub}}|, \\ \text{s.t. } |\phi(\mathcal{G}^{\text{sub}}) - \phi(\mathcal{G})| < \delta_1 \text{ and } \mathcal{L}_{\text{align}}(\mathcal{G}^{\text{sub}}) < \delta_2 \end{aligned} \quad (3)$$

where  $\mathcal{E}_p$  is the set of edges to be pruned and  $\mathcal{L}_{\text{align}}$  is the modality semantic alignment loss.  $\delta_1$  and  $\delta_2$  define the allowable thresholds.

## 4. The Proposed M<sup>3</sup>Prune Framework

Fig. 2 illustrates our M<sup>3</sup>Prune framework, comprising three primary components: Intra-modal Graph Sparsification (▷ Section 4.1), Inter-modal Graph Sparsification (▷ Section 4.2), and Progressive Edge Pruning (▷ Section 4.3).

### 4.1. Intra-Modal Graph Sparsification

We design a spatio-temporal message-passing technique to facilitate effective interaction of task viewpoints among agents in both visual and textual modalities. To improve the final response quality, we dynamically adjust edge weights

<sup>4</sup>We employ topological sorting to ensure that the graph structure forms a Directed Acyclic Graph (DAG) [5].

between agents and sparsifies redundant connections to focus on critical interactions.

**Edge Weight Initialization.** Given the predefined spatial and temporal edges  $\mathcal{E}_m^{\mathcal{S}}$  and  $\mathcal{E}_m^{\mathcal{T}}$  for  $m \in \{\text{txt, vis}\}$  across different modalities, we obtain the initial adjacency matrices  $\mathbf{A}_m^{\mathcal{S}}$  and  $\mathbf{A}_m^{\mathcal{T}}$ . We then define  $\mathcal{A}_{\text{intra}} = \bigcup_{m \in \{\text{txt, vis}\}} \bigcup_{\mathcal{X} \in \{\mathcal{S}, \mathcal{T}\}} \mathbf{A}_m^{\mathcal{X}}$ , where  $\mathcal{A}_{\text{intra}} \in \{0, 1\}^{N_m \times N_m}$  and  $N_m$  is the number of agents in modality  $m$ . Based on this adjacency matrix, we initialize trainable logits  $\tilde{\mathbf{A}}_m^{\mathcal{S}}$  and  $\tilde{\mathbf{A}}_m^{\mathcal{T}}$  in the range  $[0, 1]$  for each edge. We also define  $\tilde{\mathcal{A}}_{\text{intra}} = \bigcup_{m \in \{\text{txt, vis}\}} \bigcup_{\mathcal{X} \in \{\mathcal{S}, \mathcal{T}\}} \tilde{\mathbf{A}}_m^{\mathcal{X}}$ , and employ Gumbel-Softmax [16] to achieve differentiable discretization:

$$\tilde{\mathcal{A}}_{\text{intra}}[i, j] = \frac{\exp((\log(\mathcal{A}_{\text{intra}}[i, j]) + g_{ij})/\tau)}{\sum_{k=1}^{N_m} \exp((\log(\mathcal{A}_{\text{intra}}[i, k]) + g_{ik})/\tau)} \quad (4)$$

where  $g_{ij} \sim \text{Gumbel}(0, 1)$  and  $\tau$  is the temperature.

**Intra-Modal Message Passing.** Based on the initial spatial adjacency matrix and spatial logits, we first perform DAG sampling on the graph to ensure sequential communication among agents:  $\hat{\mathcal{G}}^{\text{intra}} \leftarrow \text{DAGSampling}(\mathcal{G}^{\text{intra}})$ . In the intra-modal graph  $\hat{\mathcal{G}}^{\text{intra}}$ , the agent  $v_i^{m, (t)}$  at round  $t$  receives the spatio-temporal information:

$$\mathcal{M}_{i, \text{intra}}^{(m, \mathcal{S}, (t))} = \sum_{v_j^{m, (t)} \in \mathcal{N}_{\text{intra}}^{\mathcal{S}}(v_i^{m, (t)})} \mathcal{W}_m^{(\mathcal{S}, (t))}[i, j] \cdot \mathcal{O}(v_j^{m, (t)}) \quad (5)$$

$$\mathcal{W}_m^{(\mathcal{S}, (t))}[i, j] = \frac{\exp(\tilde{\mathbf{A}}_m^{(\mathcal{S}, (t))}[i, j])}{\sum_{v_k^{m, (t)} \in \mathcal{N}_{\text{intra}}^{\mathcal{S}}(v_i^{m, (t)})} \exp(\tilde{\mathbf{A}}_m^{(\mathcal{S}, (t))}[i, k])} \quad (6)$$

where  $m \in \{\text{txt, vis}\}$ ,  $\mathcal{N}_{\text{intra}}^{\mathcal{S}}(v_i^{m, (t)})$  is the set of all spatial predecessor nodes of  $v_i^{m, (t)}$  at round  $t$  (only containing intra-modal agents), and  $\mathcal{O}(v_j^{m, (t)})$  represents the output content of node  $v_j^{m, (t)}$  at round  $t$ . Since the current agent  $v_i^{m, (t)}$  may be connected to multiple neighbors, their messages contribute differentially to its reasoning. Therefore, we employ Eq. 6 to compute their aggregation weights. This applies to the spatial neighboring message  $\mathcal{M}_{i, \text{intra}}^{(m, \mathcal{S}, (t))}$  and likewise to the temporal neighboring information. Each node aggregates spatio-temporal information and leverages the MLLM to generate its response. After  $T$  rounds of discussion, a dedicated decision agent synthesizes messages from all modalities to produce the final answer.

**Intra-Modal Edge Optimization.** The training objective for edge optimization, which reformulates Eq. 3, is to ensure that the adjacency matrix reflects active communication edges and the connection logits represent the contribution of interactions, thereby balancing overall task performance and graph sparsity:

$$\text{argmax}_{\tilde{\mathbf{A}}_m^{\mathcal{S}}, \tilde{\mathbf{A}}_m^{\mathcal{T}}} \mathbb{E}_{\hat{\mathcal{G}}^{\text{intra}}} [\phi(\hat{\mathcal{G}}^{\text{intra}})] - \sum_{\mathcal{X} \in \{\mathcal{S}, \mathcal{T}\}} \text{rank}(\tilde{\mathbf{A}}_m^{\mathcal{X}}) \quad (7)$$

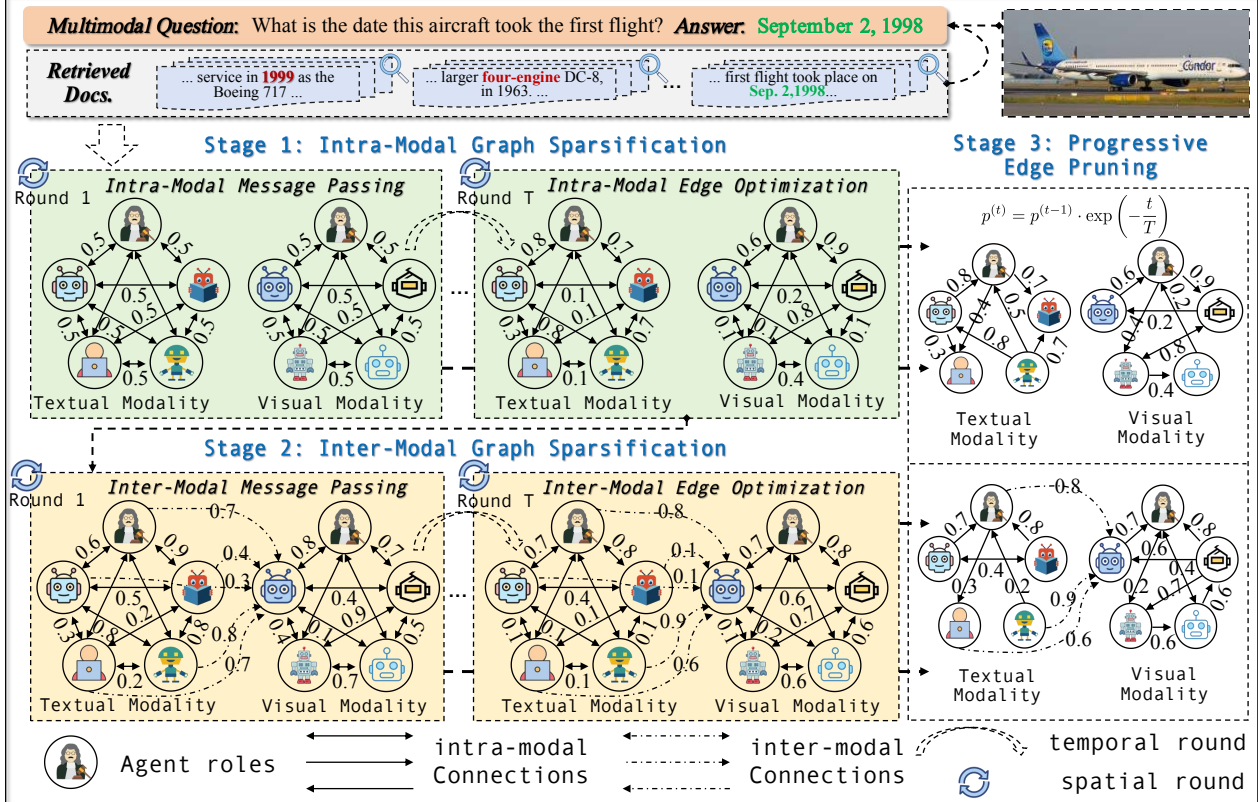


Figure 2. Overview of  $M^3$ Prune. Key components include: (1) Intra-modal Graph Sparsification: analyzes the input question using the multi-agent structures of textual and visual modalities, respectively; (2) Inter-modal Graph Sparsification: supplements semantic information across modalities through the interaction of multi-agent viewpoints in textual and visual modalities; (3) Progressive Edge Pruning: prunes redundant edges in each round of the learning process. Due to the numerous connections between agents in the inter-modal stage, we illustrate the interaction of only one agent with dashed lines as an example.

on condition that  $\sum_{\mathcal{X} \in \{\mathcal{S}, \mathcal{T}\}} \|\mathbf{A}_m^{\mathcal{X}} - \tilde{\mathbf{A}}_m^{\mathcal{X}}\|_F \leq \epsilon$ , where  $\epsilon$  defines the noise level, and  $\phi(\cdot)$  is the task performance evaluation metric. Because the employed MLLMs may rely on non-differentiable APIs, we leverage the policy gradient method [46] to approximate the objective:

$$\nabla \mathbb{E}_{\hat{\mathcal{G}}^{\text{intra}}}[\phi(\hat{\mathcal{G}}^{\text{intra}})] \approx \frac{1}{K} \sum_{k=1}^K \phi(\hat{\mathcal{G}}_k^{\text{intra}}) \cdot \nabla \log \mathcal{P}(\hat{\mathcal{G}}_k^{\text{intra}}) \quad (8)$$

where  $\mathcal{P}(\hat{\mathcal{G}}_k^{\text{intra}}) = \left( \prod_{t=1}^T \prod_{e_{ij} \in \mathcal{E}_m^{\mathcal{S}, k, (t)}} \tilde{\mathbf{A}}_m^{\mathcal{S}, (t)}[i, j] \right) \cdot \left( \prod_{t=2}^T \prod_{e_{ij} \in \mathcal{E}_m^{\mathcal{T}, k, (t)}} \tilde{\mathbf{A}}_m^{\mathcal{T}, (t)}[i, j] \right)$  is the sampling probability for graph  $\hat{\mathcal{G}}_k^{\text{intra}}$  and  $K$  is the total number of sampling graphs. For the second term, we replace the rank function with the nuclear norm [52] to address the NP-hardness of rank minimization, i.e.,  $\text{argmin}_{\tilde{\mathbf{A}}_m^{\mathcal{S}}, \tilde{\mathbf{A}}_m^{\mathcal{T}}} \sum_{\mathcal{X} \in \{\mathcal{S}, \mathcal{T}\}} \|\tilde{\mathbf{A}}_m^{\mathcal{X}}\|_*$  where  $\|\cdot\|_*$  denotes the sum of singular values of a matrix.

## 4.2. Inter-Modal Graph Sparsification

Building on intra-modal graphs, we integrate cross-modal information and learn the importance of cross-modal edges. This topology is optimized for both task performance and

structural regularity. In addition, a modality alignment loss is introduced to ensure consistent task understanding across modalities during the sparsification process.

**Inter-Modal Message Passing.** The intra-modal edges  $(\mathcal{E}_m^{\mathcal{S}}, \mathcal{E}_m^{\mathcal{T}})$ , adjacency matrices  $(\mathbf{A}_m^{\mathcal{S}}, \mathbf{A}_m^{\mathcal{T}})$ , and edge logits  $(\tilde{\mathbf{A}}_m^{\mathcal{S}}, \tilde{\mathbf{A}}_m^{\mathcal{T}})$  are initialized based on the training results of the previous intra-modal phase. Given predefined inter-modal spatial edges  $\mathcal{E}_{m'}^{\mathcal{S}}$  and temporal edges  $\mathcal{E}_{m'}^{\mathcal{T}}$ , each agent is connected to all cross-modal agents, where  $m' \in \{\text{txt} \rightarrow \text{vis}, \text{vis} \rightarrow \text{txt}\}$  denotes the two types of inter-modality. We obtain the initial inter-modal adjacency matrices  $\mathbf{A}_{m'}^{\mathcal{S}}$  and  $\mathbf{A}_{m'}^{\mathcal{T}}$ . Similarly, we employ Gumbel-Softmax to initialize the inter-modal edge logits  $\tilde{\mathbf{A}}_{m'}^{\mathcal{S}}$  and  $\tilde{\mathbf{A}}_{m'}^{\mathcal{T}}$  using Eq. 4. We then define the adjacency matrix set  $\mathcal{A}_{\text{inter}} = \bigcup_{m'} \bigcup_{\mathcal{X} \in \{\mathcal{S}, \mathcal{T}\}} \mathbf{A}_{m'}^{\mathcal{X}}$ , and the edge logits set  $\tilde{\mathcal{A}}_{\text{inter}} = \bigcup_{m'} \bigcup_{\mathcal{X} \in \{\mathcal{S}, \mathcal{T}\}} \tilde{\mathbf{A}}_{m'}^{\mathcal{X}}$ . We perform DAG sampling with  $\hat{\mathcal{G}}_{\text{inter}} \leftarrow \text{DAGSampling}(\mathcal{G}_{\text{inter}})$  to maintain the graph's topological order. Each agent  $v_i^{(t)}$  at round  $t$  receives neighboring information, including spatio-temporal

Training Paradigms	Baselines	Llama3.2-VL (11B)														Qwen-VL-Max													
		Subject			Context Modality			Grade		Avg.	Subject			Context Modality			Grade		Avg.										
		NAT	Soc	LAN	TXT	IMG	NO	G1-6	G7-12		NAT	Soc	LAN	TXT	IMG	NO	G1-6	G7-12											
Zero-shot	SP CoT	82.92 84.89	88.79 <b>97.95</b>	77.55 69.00	82.87 85.88	82.47 <b>93.70</b>	79.09 70.51	84.30 87.36	79.99 76.59	82.76 $\pm$ 1.2 83.51 $\pm$ 0.5	91.90 92.36	90.56 91.56	89.36 90.45	91.47 91.64	88.09 88.99	90.99 91.99	91.44 92.03	90.10 91.10	90.96 $\pm$ 0.9 91.70 $\pm$ 0.8										
Single-agent RAG	Wiki-LLaVA	82.30	92.21	80.25	83.69	84.66	80.21	84.80	82.17	83.85 $\pm$ 0.8	91.00	95.62	89.98	91.84	91.45	89.44	93.13	89.10	91.69 $\pm$ 0.4										
	RoRA-VLM	82.23	92.11	80.20	83.64	84.61	80.13	84.77	82.13	83.80 $\pm$ 0.9	90.92	95.51	89.88	91.78	91.40	89.39	93.04	89.07	91.65 $\pm$ 1.5										
	EchoSight	82.35	92.23	80.27	83.70	84.69	80.23	84.81	82.21	83.88 $\pm$ 1.1	91.04	95.65	90.00	91.87	91.47	89.48	93.19	89.12	91.73 $\pm$ 0.8										
	LLaVA-mR2AG	82.37	92.22	80.31	83.73	84.71	80.26	84.85	82.23	83.90 $\pm$ 0.8	91.07	95.68	90.02	91.90	91.48	89.51	93.22	89.17	91.80 $\pm$ 0.6										
Mutli-agent RAG	CoRe-MMRAG	82.44	92.31	80.30	83.77	84.73	80.28	84.86	82.27	83.94 $\pm$ 1.2	91.10	95.72	90.06	91.93	91.50	89.55	93.24	89.18	91.82 $\pm$ 1.0										
	OmniSearch	82.71	88.13	<b>83.36</b>	82.61	80.56	83.33	85.25	81.80	84.01 $\pm$ 0.3	92.50	93.43	90.09	93.35	91.31	89.71	93.35	89.76	92.07 $\pm$ 0.4										
	ViDoRAG	83.88	92.15	83.00	83.97	84.96	82.39	87.43	81.72	85.39 $\pm$ 0.7	93.99	92.20	90.45	93.91	90.26	91.29	93.79	90.74	92.70 $\pm$ 0.5										
	HM-RAG	<b>86.25</b>	94.89	72.45	<b>86.56</b>	<b>89.70</b>	75.23	87.78	79.45	84.80 $\pm$ 1.3	94.30	93.66	92.36	93.47	90.36	94.08	94.15	92.78	93.66 $\pm$ 1.2										
	E-Agent	83.00	87.58	83.09	82.45	80.40	83.51	85.31	81.59	83.98 $\pm$ 1.4	93.67	93.44	89.18	94.06	91.84	89.90	93.20	91.13	92.46 $\pm$ 1.5										
	<b>Ours</b>	85.97	94.60	81.45	85.29	86.47	<b>83.83</b>	<b>88.25</b>	<b>83.65</b>	<b>86.61<math>\pm</math>0.6</b>	<b>97.51</b>	<b>96.63</b>	<b>97.82</b>	<b>97.70</b>	<b>96.13</b>	<b>97.98</b>	<b>98.05</b>	<b>96.24</b>	<b>97.41<math>\pm</math>0.4</b>										

Table 1. Performance comparison between M<sup>3</sup>Prune and baselines on domain-specific ScienceQA task.

data from both modalities via  $\hat{\mathcal{G}}^{\text{inter}}$ :

$$\mathcal{M}_{i,\text{inter}}^{\mathcal{S},(t)} = \sum_{v_j^{(t)} \in \mathcal{N}_{\text{inter}}^{\mathcal{S}}(v_i^{(t)})} \mathcal{W}^{(\mathcal{S},(t))}[i, j] \cdot \mathcal{O}(v_j^{(t)}) \quad (9)$$

$$\mathcal{W}^{(\mathcal{S},(t))}[i, j] = \frac{\exp(\tilde{\mathcal{A}}^{(\mathcal{S},(t))}[i, j])}{\sum_{v_k^{(t)} \in \mathcal{N}_{\text{inter}}^{\mathcal{S}}(v_i^{(t)})} \exp(\tilde{\mathcal{A}}^{(\mathcal{S},(t))}[i, k])} \quad (10)$$

where  $\mathcal{N}_{\text{inter}}^{\mathcal{S}}(v_i^{(t)})$  is the set of all spatial predecessor nodes of  $v_i^{(t)}$  at round  $t$ , containing both types of agents.  $\tilde{\mathcal{A}} = \tilde{\mathcal{A}}_{\text{intra}} \cup \tilde{\mathcal{A}}_{\text{inter}}$  denotes the overall intra- and inter-edge logits. We also employ Eq. 10 to compute aggregation weights, analogous to Eq. 6. Each node aggregates spatio-temporal information from both modalities and uses the MLLM to generate its output response. After  $T$  rounds of multi-agent discussion, our model employs a decision agent to synthesize messages from all agents and generate the final answer.

**Inter-Modal Edge Optimization.** Similar to intra-modal edge optimization, our training objective must ensure both task performance and graph sparsity. In addition, we introduce a modality alignment loss to unify semantic understanding across different modalities by enforcing alignment constraints and preserving inter-modal associations:

$$\begin{aligned} & \arg \max_{\tilde{\mathcal{A}}_{\text{inter}}} \mathbb{E}_{\tilde{\mathcal{G}}_{\text{inter}}} [\phi(\hat{\mathcal{G}}^{\text{inter}})] - \text{rank}(\tilde{\mathcal{A}}_{\text{inter}}) \\ & + \sum_{\mathcal{X} \in \{\mathcal{S}, \mathcal{T}\}} \mathcal{L}_{\text{align}}(\tilde{\mathbf{A}}_{\text{txt} \rightarrow \text{vis}}^{\mathcal{X}}, \tilde{\mathbf{A}}_{\text{vis} \rightarrow \text{txt}}^{\mathcal{X}}) \end{aligned} \quad (11)$$

on condition that  $\sum_{\mathcal{X} \in \{\mathcal{S}, \mathcal{T}\}} \|\mathbf{A}_{\text{txt} \rightarrow \text{vis}}^{\mathcal{X}} - \tilde{\mathbf{A}}_{\text{txt} \rightarrow \text{vis}}^{\mathcal{X}}\|_F \leq \epsilon'$  and  $\sum_{\mathcal{X} \in \{\mathcal{S}, \mathcal{T}\}} \|\mathbf{A}_{\text{vis} \rightarrow \text{txt}}^{\mathcal{X}} - \tilde{\mathbf{A}}_{\text{vis} \rightarrow \text{txt}}^{\mathcal{X}}\|_F \leq \epsilon'$ . The modality alignment loss is defined as:

$$\begin{aligned} & \mathcal{L}_{\text{align}}(\tilde{\mathbf{A}}_{\text{txt} \rightarrow \text{vis}}^{\mathcal{X}}, \tilde{\mathbf{A}}_{\text{vis} \rightarrow \text{txt}}^{\mathcal{X}}) = \\ & -\frac{1}{N_T N_I} \sum_i \left( 1 - \frac{\tilde{\mathbf{A}}_{\text{txt} \rightarrow \text{vis}}^{\mathcal{X}}[i, :] \cdot [\tilde{\mathbf{A}}_{\text{vis} \rightarrow \text{txt}}^{\mathcal{X}}]^T[i, :]}{\|\tilde{\mathbf{A}}_{\text{txt} \rightarrow \text{vis}}^{\mathcal{X}}[i, :]\| \cdot \|[\tilde{\mathbf{A}}_{\text{vis} \rightarrow \text{txt}}^{\mathcal{X}}]^T[i, :]\|} \right) \end{aligned} \quad (12)$$

where  $\epsilon'$  is the noise level.  $N_T$  and  $N_I$  represent the number of text and visual agents, respectively.

### 4.3. Progressive Edge Pruning

Our hierarchical pruning operates in two distinct stages: it first sparsifies intra-modal edges within each modality, and then proceeds to prune inter-modal connections between the textual and visual streams. This results in a progressive pruning strategy whereby the pruning rate decays over rounds, progressively increasing sparsity.

$$\mathcal{B}_{\text{intra}}^{(t)} = \mathbb{1} \left( \mathcal{A}_{\text{intra}}^{(t)} \neq 0 \wedge \text{Top}K \left( \tilde{\mathcal{A}}_{\text{intra}}^{(t)}, |\mathcal{A}_{\text{intra}}^{(t)}| \times (1 - p^{(t)}) \right) \right) \quad (13)$$

$$\mathcal{B}_{\text{inter}}^{(t)} = \mathbb{1} \left( \mathcal{A}_{\text{inter}}^{(t)} \neq 0 \wedge \text{Top}K \left( \tilde{\mathcal{A}}_{\text{inter}}^{(t)}, |\mathcal{A}_{\text{inter}}^{(t)}| \times (1 - p^{(t)}) \right) \right) \quad (14)$$

where  $\mathbb{1}$  is the indicator function and  $\text{Top}K$  selects the largest  $(1 - p^{(t)})$  fraction of elements in the matrix.  $p^{(t)} = p^{(t-1)} \cdot \exp(-\frac{t}{T})$  is the pruning rate at round  $t$ . Here,  $\mathcal{B}$  is an indicator matrix: a zero entry indicates that the corresponding element in the adjacency matrix should be set to 0, and a one entry indicates that it should remain 1. After each discussion round, the adjacency matrices are updated as:  $\mathcal{A}_{\text{intra}}^{(t+1)} = \mathcal{A}_{\text{intra}}^{(t)} \odot \mathcal{B}_{\text{intra}}^{(t)}$  and  $\mathcal{A}_{\text{inter}}^{(t+1)} = \mathcal{A}_{\text{inter}}^{(t)} \odot \mathcal{B}_{\text{inter}}^{(t)}$ , where  $\odot$  denotes element-wise multiplication. A detailed description of the training algorithm pipeline is provided in Appendix 9.

## 5. Experiments

Due to space limitations, we describe datasets, baselines, and implementation details in Appendix 8. Other experiments including pruning rate analysis, hyperparameters analysis and case study are shown in Appendix 10.

### 5.1. Main Results

We evaluate M<sup>3</sup>Prune against three categories of baselines on both general and domain-specific multi-modal QA tasks, with results summarized in Table 1 and Table 2. we can observe that (1) Standard prompting (SP) and CoT exhibit limited performance due to the absence of external knowledge. (2) Single-agent RAG methods consistently outperform

Backbone	Training Paradigms	Baselines	Vidoseek												MultimodalQA				Average			
			Single-hop		Multi-hop		Text		Table		Chart		Layout		Image		Text					
			Acc*	EM	Acc*	EM	Acc*	EM	Acc*	EM	Acc*	EM	Acc*	EM	Acc*	EM	Acc*	EM				
Llama3.2-VL (11B)	Single-agent RAG	Zero-shot	SP CoT	25.89 30.61	2.48 5.17	12.07 7.44	8.45 9.24	26.25 21.00	0.01 4.25	9.14 10.14	5.14 5.86	14.65 9.92	10.83 13.83	22.88 25.25	4.38 6.01	14.68 16.82	15.23 15.68	36.28 33.42	31.46 32.53	$20.23 \pm 0.8$ $19.33 \pm 1.3$	$9.75 \pm 0.6$ $11.57 \pm 1.1$	
		Wiki-LLaVA		47.35	16.94	46.16	36.72	48.88	11.37	38.38	29.20	37.61	31.88	50.61	24.83	13.01	12.11	58.10	49.95	$42.51 \pm 0.5$	$26.63 \pm 0.8$	
		RoRA-VLM		47.25	16.83	46.05	36.55	48.66	11.20	38.21	29.03	37.44	31.81	50.43	24.71	12.91	11.49	57.91	49.67	$42.37 \pm 1.5$	$26.41 \pm 1.2$	
		EchoSight		47.29	16.90	46.08	36.62	48.75	11.25	38.29	29.14	37.58	31.85	50.55	24.79	12.95	11.59	57.97	49.75	$42.43 \pm 0.5$	$26.49 \pm 0.4$	
		LLaVA-mR2AG		47.63	17.23	46.45	36.92	48.97	11.43	38.89	29.45	37.74	31.99	50.87	24.99	12.99	11.76	58.13	49.98	$42.71 \pm 0.9$	$26.72 \pm 0.7$	
	Mutli-agent RAG	CoRe-MMRAG		47.53	17.23	46.34	36.85	48.98	11.44	38.41	29.54	37.87	31.96	50.78	24.96	13.14	12.42	58.25	50.04	$42.66 \pm 1.2$	$26.81 \pm 1.3$	
		OmniSearch		48.83	17.95	45.61	37.00	44.75	16.50	41.29	30.29	<b>40.94</b>	<b>38.39</b>	50.59	23.73	17.27	17.50	58.23	51.14	$43.44 \pm 0.8$	$29.06 \pm 0.7$	
		ViDoRAG		49.37	<b>20.61</b>	45.55	36.75	56.00	<b>23.50</b>	41.57	27.00	38.20	32.02	50.32	27.30	20.23	18.64	64.30	56.33	$45.69 \pm 1.0$	$30.27 \pm 1.1$	
		HM-RAG		<b>56.72</b>	20.22	34.33	32.52	<b>56.75</b>	19.50	37.00	30.29	34.02	33.66	<b>51.08</b>	23.37	<b>31.77</b>	24.09	53.84	49.11	$44.44 \pm 1.5$	$29.10 \pm 0.9$	
		E-Agent		48.06	18.04	44.47	37.21	48.75	16.75	38.29	28.71	37.58	34.85	50.14	25.05	23.55	21.05	64.38	56.15	$44.40 \pm 0.6$	$29.73 \pm 0.9$	
		<b>Ours</b>		44.65	19.38	<b>54.12</b>	<b>42.25</b>	51.25	12.50	<b>48.57</b>	<b>37.71</b>	40.13	34.39	50.41	<b>28.08</b>	29.55	<b>28.41</b>	<b>73.16</b>	<b>64.56</b>	$48.98 \pm 0.7$	$33.41 \pm 0.8$	
Qwen-VL-Max	Single-agent RAG	Zero-shot	SP CoT	39.84 45.89	4.65 5.41	13.28 15.29	8.25 11.05	36.25 43.75	0.01 3.25	13.14 12.57	7.43 6.57	21.02 26.11	14.01 16.65	32.60 37.53	4.93 6.79	35.00 32.27	30.23 27.73	51.65 53.92	43.29 44.94	$30.35 \pm 0.6$	$14.10 \pm 0.4$	
		Wiki-LLaVA		53.91	19.89	49.91	40.81	57.11	12.39	47.10	37.01	46.27	39.22	55.70	26.58	24.30	22.21	69.73	60.42	$50.50 \pm 1.2$	$32.32 \pm 1.1$	
		RoRA-VLM		55.45	20.00	50.41	40.99	57.40	12.43	47.38	37.10	46.42	39.36	55.89	26.69	24.25	22.24	69.85	60.56	$50.88 \pm 1.3$	$32.42 \pm 0.8$	
		EchoSight		55.81	20.16	50.50	41.05	57.50	12.50	47.43	37.14	46.50	39.49	56.03	26.99	24.32	22.27	69.87	60.63	$51.00 \pm 0.6$	$32.53 \pm 0.5$	
		LLaVA-mR2AG		55.97	20.34	50.82	41.49	57.63	12.74	47.83	37.33	46.69	39.61	56.46	27.21	24.84	22.61	69.99	60.91	$51.28 \pm 0.9$	$32.78 \pm 1.0$	
	Mutli-agent RAG	CoRe-MMRAG		55.82	20.29	50.75	41.36	57.54	12.64	47.71	37.30	46.59	39.58	56.33	27.10	24.61	22.40	69.91	60.88	$51.16 \pm 1.1$	$32.69 \pm 1.5$	
		OmniSearch		59.84	20.38	50.91	42.85	61.25	14.75	44.57	35.86	49.04	43.04	59.59	27.71	33.05	29.18	78.03	68.66	$54.54 \pm 1.3$	$35.30 \pm 1.7$	
		ViDoRAG		68.43	22.29	58.73	48.67	84.25	29.00	50.43	40.57	60.96	53.04	66.01	28.52	30.68	30.45	82.41	74.30	$62.74 \pm 0.8$	$40.86 \pm 1.1$	
		HM-RAG		66.88	20.71	52.50	46.03	68.00	20.50	49.29	39.43	47.59	44.94	65.33	28.27	36.09	33.45	78.27	69.27	$57.99 \pm 1.0$	$37.83 \pm 0.9$	
		E-Agent		68.27	22.67	52.30	43.03	64.25	17.50	49.29	37.00	49.50	44.49	66.42	28.97	41.45	38.36	83.15	74.03	$59.33 \pm 0.6$	$38.26 \pm 0.8$	
		<b>Ours</b>		<b>73.95</b>	<b>26.67</b>	<b>68.41</b>	<b>56.54</b>	<b>85.00</b>	<b>30.00</b>	<b>64.57</b>	<b>53.14</b>	<b>63.06</b>	<b>56.05</b>	<b>73.56</b>	<b>33.97</b>	<b>70.23</b>	<b>70.00</b>	<b>86.08</b>	<b>78.10</b>	<b>73.11 <math>\pm 0.7</math></b>	<b>50.56 <math>\pm 0.9</math></b>	

Table 2. Performance comparison between  $M^3$ Prune and baseline methods on general-domain multi-modal QA tasks. Due to the space limitation, we present the performance on Qwen2.5-VL (7B) in Appendix 10.1.

form zero-shot approaches, validating the importance of retrieved contexts. (3) Multi-agent RAG frameworks generally surpass single-agent counterparts, suggesting that discussions among multiple agents facilitate exchange of viewpoints and help mitigate errors in single-agent retrieval. (4)  $M^3$ Prune achieves superior performance compared to fixed-topology multi-agent methods across both general and domain-specific tasks, indicating that our intra-modal and inter-modal pruning techniques effectively eliminate redundant agent roles and prevent these viewpoints from introducing noise that could disrupt productive discussions. (5)  $M^3$ Prune’s performance advantage remains consistent across all three backbone models of varying scales (from 7B to closed-source MLLMs), demonstrating the generalizability of our approach regardless of the underlying MLLMs.

## 5.2. Ablation Study

In Table 3, we present an ablation study to analyze the contribution of key components of  $M^3$ Prune. (1) *w/o*  $\mathcal{L}_{\text{align}}$ : Removing the modality alignment loss leads to clear performance degradation, underscoring its critical role in harmonizing textual and visual representations for inter-modal collaboration. (2) *w/o*  $\hat{\mathcal{G}}^{\text{inter}}$ : Omitting inter-modal graph pruning results in naive concatenation of intra-modal outputs. The observed performance drop confirms that deep semantic integration through structured inter-modal communication is indispensable for coherent multi-modal reasoning. (3) *w/o*  $\hat{\mathcal{G}}^{\text{intra}}$ : We ablate intra-modal pruning graphs by replacing each modality’s agents with dummy outputs (e.g., a fixed response: “This is a dummy agent with no information”).

Dataset → Models ↓	MultimodalQA	ScienceQA	Average
<b>Base model: Llama3.2-VL-11B</b>			
<b>M<sup>3</sup>Prune</b>	53.14	86.61	69.88
w/o $\mathcal{L}_{\text{align}}$	50.23	84.04	67.14
w/o $\hat{\mathcal{G}}^{\text{inter}}$	50.44	82.61	66.53
w/o $\hat{\mathcal{G}}^{\text{intra}}_{\text{-txt}}$	48.78	83.56	66.17
w/o $\hat{\mathcal{G}}^{\text{intra}}_{\text{-vis}}$	51.81	80.24	66.03
<b>Base model: Qwen-VL-Max</b>			
<b>M<sup>3</sup>Prune</b>	76.40	97.41	86.91
w/o $\mathcal{L}_{\text{align}}$	74.13	95.56	84.85
w/o $\hat{\mathcal{G}}^{\text{inter}}$	73.85	94.27	84.06
w/o $\hat{\mathcal{G}}^{\text{intra}}_{\text{-txt}}$	70.91	95.69	83.30
w/o $\hat{\mathcal{G}}^{\text{intra}}_{\text{-vis}}$	74.83	92.06	83.45

Table 3. Ablation study of  $M^3$ Prune. “ $\hat{\mathcal{G}}^{\text{intra}}_{\text{-txt}}$ ” and “ $\hat{\mathcal{G}}^{\text{intra}}_{\text{-vis}}$ ” denote the ablation of intra-modalities.

tion.”). Results confirm that both modalities are indispensable, as ablating either one causes significant performance degradation. The greater sensitivity of MultimodalQA to text agents and of ScienceQA to visual agents reflects their distinct task characteristics.

## 5.3. Detailed Analysis

**Communication Edge Evolving.** To quantitatively validate the evolution of our communication topology during training, we analyze the edge weights across temporal discussion rounds in our inter-modal graph. Specifically, we

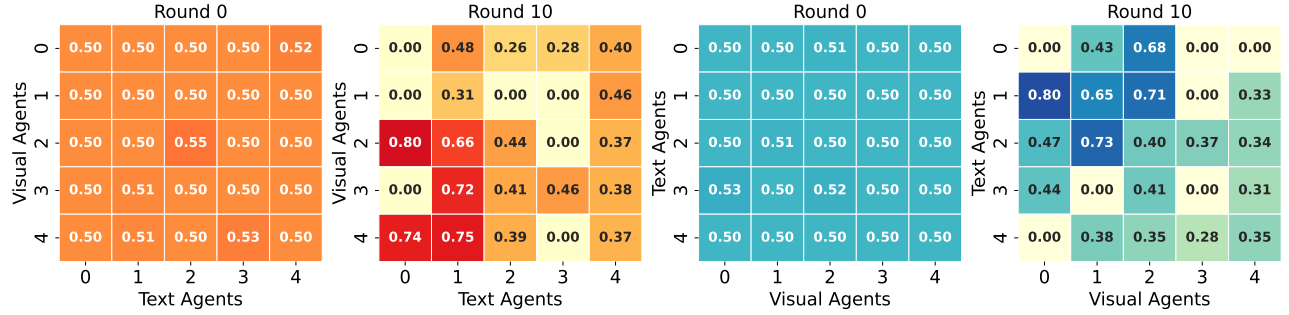


Figure 3. The process of weights change in communication edge of visual-to-text (Left) and text-to-visual (Right) on ScienceQA.

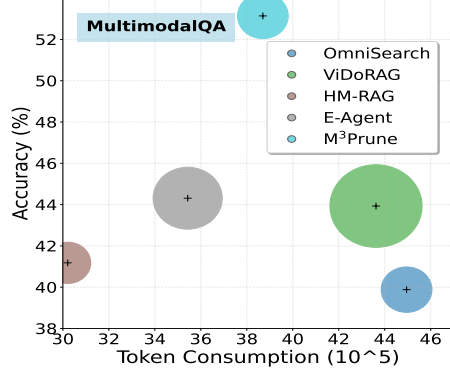


Figure 4. Comparison of the trade-off between performance and token consumption for multi-agent models. The total token count is calculated as the sum of prompt tokens and completion tokens.

track the evolution of edge weights between visual-to-text (Fig. 3, Left) and text-to-visual (Fig. 3, Right) agents on ScienceQA using Qwen-VL-Max. The complete evolution process is detailed in Appendix 10.3.

As shown in Fig. 3, we observe that this emerging weight differentiation demonstrates two key properties: (1) Our model develops increasingly strong preferences for certain inter-agent connections as reasoning deepens, as reflected in the dark-colored blocks. (2) The hierarchical communication graph pruning of low-correlation edges progressively sparsifies the graph, evidenced by the gradual lightening of non-essential connections. These findings confirm that our model successfully learns to identify and reinforce semantically meaningful communication patterns while eliminating redundant interactions.

**Trade-off between Performance and Token Cost.** To assess the cost-effectiveness of our framework, we analyze the trade-off between performance gains and token consumption across all agents using the MultimodalQA, Vidoseek, and ScienceQA tasks on Llama-3.2-VL-11B. The overall token consumption analysis is provided in Appendix 10.4.

As shown in Fig. 4, M<sup>3</sup>Prune achieves superior performance with only a moderate increase in token usage. This balance stems from our adaptive hierarchical graph pruning strategy, which selectively retains meaningful agent com-

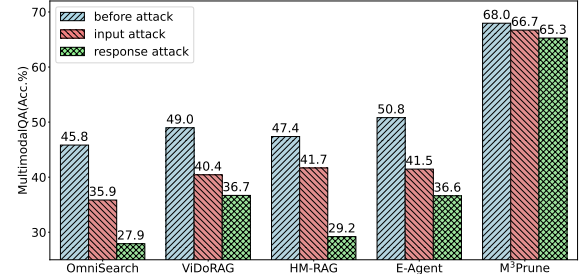


Figure 5. Performance under adversarial attacks, including input prompt and response perturbations on MultimodalQA.

munication groups while eliminating redundant and noisy edges. In contrast, baseline methods with fixed-topology agent structures based on heuristic or iterative communication patterns achieve slightly lower token usage at the cost of substantially reduced performance.

**Robustness Verification.** This experiment aims to verify whether our model maintains stable performance when critical agents are attacked compared to fixed-topology baselines. Specifically, we evaluate the methods on MultimodalQA using Qwen2.5-VL-7B under two attack scenarios: (1) *Input Prompt Attack*: Replacing one original agent with a malicious agent that ignores all inter-modal agent communications and relies solely on its own knowledge. (2) *Response Attack*: Substituting one agent with an adversarial agent that intentionally generates incorrect answers and misleading explanations to disrupt other agents' reasoning processes. As shown in Fig. 5, existing multi-agent baselines with fixed topology exhibit significant performance degradation under both attack types due to their inability to dynamically reweight interactions or redistribute role-specific loads. In contrast, M<sup>3</sup>Prune maintains stable performance by adaptively pruning and reweighting edges, thereby dynamically isolating the compromised agents.

## 6. Conclusion

In this paper, we introduce M<sup>3</sup>Prune, a novel framework for multi-modal multi-agent systems that dynamically optimizes agent connections through structured pruning. Our method systematically addresses the critical challenge of

redundant communication in collaborative reasoning by proposing progressive pruning mechanisms for intra-modal and inter-modal hierarchical graphs. This two-stage approach enables agents to first establish robust, task-specific perspectives within individual modalities, before engaging in semantically complementary interactions across modalities. Extensive experiments on both general-domain and domain-specific benchmarks demonstrate that our framework achieves state-of-the-art performance while maintaining significantly higher token efficiency.

## References

- [1] Pravallika Abbineni, Saoud Aldowaish, Colin Liechty, Soroosh Noorzad, Ali Ghazizadeh, and Morteza Fayazi. Muallm: A multimodal large language model agent for circuit design assistance with hybrid contextual retrieval-augmented generation. *CoRR*, abs/2508.08137, 2025. 3
- [2] Mohammad Mahdi Abootorabi, Amirhosein Zobeiri, Mahdi Dehghani, Mohammadali Mohammadkhani, Bardia Mammadi, Omid Ghahroodi, Mahdieh Soleymani Baghshah, and Ehsaneddin Asgari. Ask in any modality: A comprehensive survey on multimodal retrieval-augmented generation. In *Findings of the Association for Computational Linguistics*, pages 16776–16809, 2025. 2, 4
- [3] Arian Askari, Emmanouil Stergiadis, Ilya Gusev, and Moran Beladev. Hotelmatch-llm: Joint multi-task training of small and large language models for efficient multimodal hotel retrieval. In *Proceedings of the Association for Computational Linguistics*, pages 607–619, 2025. 1
- [4] Shuai Bai, Kebin Chen, Xuejing Liu, Jialin Wang, Wenbin Ge, Sibo Song, Kai Dang, Peng Wang, Shijie Wang, Jun Tang, et al. Qwen2. 5-vl technical report. *arXiv preprint arXiv:2502.13923*, 2025. 3
- [5] John Adrian Bondy, Uppaluri Siva Ramachandra Murty, et al. *Graph theory with applications*. Macmillan London, 1976. 4
- [6] Davide Caffagni, Federico Cocchi, Nicholas Moratelli, Sara Sarto, Marcella Cornia, Lorenzo Baraldi, and Rita Cucchiara. Wiki-llava: Hierarchical retrieval-augmented generation for multimodal llms. In *IEEE/CVF Conference on Computer Vision and Pattern Recognition*, pages 1818–1826, 2024. 3
- [7] Qi Cai, Yingwei Pan, Ting Yao, Chong-Wah Ngo, and Tao Mei. Objectfusion: Multi-modal 3d object detection with object-centric fusion. In *IEEE/CVF International Conference on Computer Vision*, pages 18021–18030, 2023. 2
- [8] Guillem Capellera, Antonio Rubio, Luis Ferraz, and Antonio Agudo. Unified uncertainty-aware diffusion for multi-agent trajectory modeling. In *IEEE/CVF Conference on Computer Vision and Pattern Recognition*, pages 22476–22486, 2025. 3
- [9] Chia-Yuan Chang, Zhimeng Jiang, Vineeth Rakesh, Menghai Pan, Chin-Chia Michael Yeh, Guanchu Wang, Mingzhi Hu, Zhichao Xu, Yan Zheng, Mahashweta Das, and Na Zou. MAIN-RAG: multi-agent filtering retrieval-augmented generation. In *Proceedings of the Association for Computational Linguistics*, pages 2607–2622, 2025. 1
- [10] Jiawei Chen, Yue Jiang, Dingkang Yang, Mingcheng Li, Jinjie Wei, Ziyun Qian, and Lihua Zhang. Can llms' tuning methods work in medical multimodal domain? In *Medical Image Computing and Computer Assisted Intervention*, pages 112–122, 2024. 1
- [11] Sanghyuk Chun, Seong Joon Oh, Rafael Sampaio de Rezende, Yannis Kalantidis, and Diane Larlus. Probabilistic embeddings for cross-modal retrieval. In *IEEE Conference on Computer Vision and Pattern Recognition*, pages 8415–8424, 2021. 3
- [12] Guanting Dong, Chenghao Zhang, Mengjie Deng, Yutao Zhu, Zhicheng Dou, and Ji-Rong Wen. Progressive multimodal reasoning via active retrieval. In *Proceedings of the Association for Computational Linguistics*, pages 3579–3602, 2025. 1
- [13] Guanting Dong, Chenghao Zhang, Mengjie Deng, Yutao Zhu, Zhicheng Dou, and Ji-Rong Wen. Progressive multimodal reasoning via active retrieval. In *Proceedings of the Association for Computational Linguistics*, pages 3579–3602, Vienna, Austria, 2025. 3
- [14] Aaron Grattafiori, Abhimanyu Dubey, Abhinav Jauhri, Abhinav Pandey, Abhishek Kadian, Ahmad Al-Dahle, Aiesha Letman, Akhil Mathur, Alan Schelten, Alex Vaughan, et al. The llama 3 herd of models. *arXiv preprint arXiv:2407.21783*, 2024. 3
- [15] Yushi Hu, Benlin Liu, Jungo Kasai, Yizhong Wang, Mari Ostendorf, Ranjay Krishna, and Noah A. Smith. TIFA: accurate and interpretable text-to-image faithfulness evaluation with question answering. In *IEEE/CVF International Conference on Computer Vision*, pages 20349–20360, 2023. 1
- [16] Eric Jang, Shixiang Gu, and Ben Poole. Categorical reparameterization with gumbel-softmax. *arXiv preprint arXiv:1611.01144*, 2016. 4
- [17] Bowen Jiang, Yangxinyu Xie, Xiaomeng Wang, Yuan Yuan, Zhuoqun Hao, Xinyi Bai, Weijie J. Su, Camillo Jose Taylor, and Tanwi Mallick. Towards rationality in language and multimodal agents: A survey. In *Proceedings of the Nations of the Americas Chapter of the Association for Computational Linguistics*, pages 3656–3675, 2025. 1, 3
- [18] Aisha Urooj Khan, Hilde Kuehne, Kevin Duarte, Chuang Gan, Niels da Vitoria Lobo, and Mubarak Shah. Found a reason for me? weakly-supervised grounded visual question answering using capsules. In *IEEE Conference on Computer Vision and Pattern Recognition*, pages 8465–8474, 2021. 1
- [19] Jungsoo Lee, Janghoon Cho, Hyojin Park, Munawar Hayat, Kyuwoong Hwang, Fatih Porikli, and Sungha Choi. Generalized contrastive learning for universal multimodal retrieval. *CoRR*, abs/2509.25638, 2025. 1
- [20] Meng-Chieh Lee, Qi Zhu, Costas Mavromatis, Zhen Han, Soji Adeshina, Vassilis N. Ioannidis, Huzefa Rangwala, and Christos Faloutsos. Hybrag: Hybrid retrieval-augmented generation on textual and relational knowledge bases. In *Proceedings of the Association for Computational Linguistics*, pages 879–893, 2025. 1
- [21] Junnan Li, Dongxu Li, Silvio Savarese, and Steven Hoi. Blip-2: Bootstrapping language-image pre-training with

frozen image encoders and large language models. In *International conference on machine learning*, pages 19730–19742. PMLR, 2023. 3

[22] Yangning Li, Yinghui Li, Xinyu Wang, Yong Jiang, Zhen Zhang, Xinran Zheng, Hui Wang, Hai-Tao Zheng, Fei Huang, Jingren Zhou, and Philip S. Yu. Benchmarking multimodal retrieval augmented generation with dynamic VQA dataset and self-adaptive planning agent. In *International Conference on Learning Representations*, 2025. 1, 3, 4

[23] Junxiong Lin, Yan Wang, Zeng Tao, Boyang Wang, Qing Zhao, Haorong Wang, Xuan Tong, Xinji Mai, Yuxuan Lin, Wei Song, Jiawen Yu, Shaoqi Yan, and Wenqiang Zhang. Adaptive multi-modal fusion of spatially variant kernel refinement with diffusion model for blind image super-resolution. In *European Conference on Computer Vision*, pages 363–380, 2024. 2

[24] Zudi Lin, Erhan Bas, Kunwar Yashraj Singh, Gurumurthy Swaminathan, and Rahul Bhotika. Relaxing contrastiveness in multimodal representation learning. In *IEEE/CVF Winter Conference on Applications of Computer Vision*, pages 2226–2235, 2023. 1

[25] Aixin Liu, Bei Feng, Bing Xue, Bingxuan Wang, Bochao Wu, Chengda Lu, Chenggang Zhao, Chengqi Deng, Chenyu Zhang, Chong Ruan, et al. Deepseek-v3 technical report. *arXiv preprint arXiv:2412.19437*, 2024. 3

[26] Hongjun Liu, Yinghao Zhu, Yuhui Wang, Yitao Long, Zeyu Lai, Lequan Yu, and Chen Zhao. Medmmv: A controllable multimodal multi-agent framework for reliable and verifiable clinical reasoning. *CoRR*, abs/2509.24314, 2025. 3

[27] Pei Liu, Xin Liu, Ruoyu Yao, Junming Liu, Siyuan Meng, Ding Wang, and Jun Ma. HM-RAG: hierarchical multi-agent multimodal retrieval augmented generation. *CoRR*, abs/2504.12330, 2025. 1, 3

[28] Pan Lu, Swaroop Mishra, Tanglin Xia, Liang Qiu, Kai-Wei Chang, Song-Chun Zhu, Oyvind Tafjord, Peter Clark, and Ashwin Kalyan. Learn to explain: Multimodal reasoning via thought chains for science question answering. In *Advances in Neural Information Processing Systems*, 2022. 2, 3

[29] Pan Lu, Swaroop Mishra, Tanglin Xia, Liang Qiu, Kai-Wei Chang, Song-Chun Zhu, Oyvind Tafjord, Peter Clark, and Ashwin Kalyan. Learn to explain: Multimodal reasoning via thought chains for science question answering. *Advances in Neural Information Processing Systems*, 35:2507–2521, 2022. 3

[30] Ziyang Luo, Pu Zhao, Can Xu, Xiubo Geng, Tao Shen, Chongyang Tao, Jing Ma, Qingwei Lin, and Daxin Jiang. Lexlip: Lexicon-bottlenecked language-image pre-training for large-scale image-text sparse retrieval. In *IEEE/CVF International Conference on Computer Vision*, pages 11172–11183, 2023. 3

[31] Ziyu Ma, Chenhui Gou, Hengcan Shi, Bin Sun, Shutao Li, Hamid Rezatofighi, and Jianfei Cai. Drvideo: Document retrieval based long video understanding. In *IEEE/CVF Conference on Computer Vision and Pattern Recognition*, pages 18936–18946, 2025. 1

[32] Tianyi Men, Zhuoran Jin, Pengfei Cao, Yubo Chen, Kang Liu, and Jun Zhao. Agent-rewardbench: Towards a unified benchmark for reward modeling across perception, planning, and safety in real-world multimodal agents. In *Proceedings of the Association for Computational Linguistics*, pages 17521–17541, 2025. 1

[33] Jingwei Peng, Jiehao Chen, Mateo Alejandro Rojas, and Meilin Zhang. Mv-core: Multimodal visual-conceptual reasoning for complex visual question answering. *CoRR*, abs/2508.07023, 2025. 1

[34] Akhil Perincherry, Jacob Krantz, and Stefan Lee. Do visual imaginations improve vision-and-language navigation agents? In *IEEE/CVF Conference on Computer Vision and Pattern Recognition*, pages 3846–3855, 2025. 1

[35] Jingyuan Qi, Zhiyang Xu, Rulin Shao, Yang Chen, Di Jin, Yu Cheng, Qifan Wang, and Lifu Huang. Rora-vlm: Robust retrieval-augmented vision language models. *CoRR*, abs/2410.08876, 2024. 3

[36] Zi Qian, Xin Wang, Xuguang Duan, Pengda Qin, Yuhong Li, and Wenwu Zhu. Decouple before interact: Multi-modal prompt learning for continual visual question answering. In *IEEE/CVF International Conference on Computer Vision*, pages 2941–2950, 2023. 1

[37] Leonardo Ranaldi, Federico Ranaldi, and Giulia Pucci. R2-MultiOmnia: Leading multilingual multimodal reasoning via self-training. In *Proceedings of the Association for Computational Linguistics (Volume 1: Long Papers)*, pages 8220–8234, Vienna, Austria, 2025. 3

[38] Alon Talmor, Ori Yoran, Amnon Catav, Dan Lahav, Yizhong Wang, Akari Asai, Gabriel Ilharco, Hannaneh Hajishirzi, and Jonathan Berant. Multimodalqa: Complex question answering over text, tables and images. *arXiv preprint arXiv:2104.06039*, 2021. 2, 3

[39] Ryota Tanaka, Taichi Iki, Taku Hasegawa, Kyosuke Nishida, Kuniko Saito, and Jun Suzuki. Vdocrag: Retrieval-augmented generation over visually-rich documents. In *IEEE/CVF Conference on Computer Vision and Pattern Recognition*, pages 24827–24837, 2025. 1

[40] Yang Tian, Fan Liu, Jingyuan Zhang, Victoria W., Yupeng Hu, and Liqiang Nie. Core-mmrag: Cross-source knowledge reconciliation for multimodal RAG. In *Proceedings of the Association for Computational Linguistics*, pages 32967–32982, 2025. 3

[41] Guohua Wang, Shengping Song, Wuchun He, and Yongsen Zheng. CMHFK: cross-modality heterogeneous knowledge fusion for weakly supervised video anomaly detection. In *Proceedings of the Association for Computational Linguistics*, pages 31594–31607, 2025. 2

[42] Qiuchen Wang, Ruixue Ding, Zehui Chen, Weiqi Wu, Shihang Wang, Pengjun Xie, and Feng Zhao. Vidorag: Visual document retrieval-augmented generation via dynamic iterative reasoning agents. *CoRR*, abs/2502.18017, 2025. 2, 3

[43] Qiuchen Wang, Ruixue Ding, Zehui Chen, Weiqi Wu, Shihang Wang, Pengjun Xie, and Feng Zhao. Vidorag: Visual document retrieval-augmented generation via dynamic iterative reasoning agents. *arXiv preprint arXiv:2502.18017*, 2025. 3

[44] Yuechen Wang, Yuming Qiao, Dan Meng, Jun Yang, Haonan Lu, Zhenyu Yang, and Xudong Zhang. Efficient agent:

Optimizing planning capability for multimodal retrieval augmented generation. *CoRR*, abs/2508.08816, 2025. 1, 3, 4

[45] Jason Wei, Xuezhi Wang, Dale Schuurmans, Maarten Bosma, Fei Xia, Ed Chi, Quoc V Le, Denny Zhou, et al. Chain-of-thought prompting elicits reasoning in large language models. *Advances in neural information processing systems*, 35:24824–24837, 2022. 3

[46] Ronald J Williams. Simple statistical gradient-following algorithms for connectionist reinforcement learning. *Machine learning*, 8(3):229–256, 1992. 5

[47] Jin Xu, Zhifang Guo, Hangrui Hu, Yunfei Chu, Xiong Wang, Jinzheng He, Yuxuan Wang, Xian Shi, Ting He, Xinfa Zhu, et al. Qwen3-omni technical report. *arXiv preprint arXiv:2509.17765*, 2025. 3

[48] Yibin Yan and Weidi Xie. Echosight: Advancing visual-language models with wiki knowledge. In *Findings of Empirical Methods in Natural Language Processing*, pages 1538–1551, 2024. 3

[49] Shuo Yang, Caren Han, Siwen Luo, and Eduard H. Hovy. MAGIC-VQA: multimodal and grounded inference with commonsense knowledge for visual question answering. In *Findings of the Association for Computational Linguistics*, pages 16967–16986, 2025. 1

[50] Xinlei Yu, Zhangquan Chen, Yudong Zhang, Shilin Lu, Ruolin Shen, Jiangning Zhang, Xiaobin Hu, Yanwei Fu, and Shuicheng Yan. Visual document understanding and question answering: A multi-agent collaboration framework with test-time scaling. *CoRR*, abs/2508.03404, 2025. 2, 3

[51] Zhengrong Yue, Shaobin Zhuang, Kunchang Li, Yanbo Ding, and Yali Wang. V-stylist: Video stylization via collaboration and reflection of MLLM agents. In *IEEE/CVF Conference on Computer Vision and Pattern Recognition*, pages 3195–3205, 2025. 1

[52] Guibin Zhang, Yanwei Yue, Zhixun Li, Sukwon Yun, Guancheng Wan, Kun Wang, Dawei Cheng, Jeffrey Xu Yu, and Tianlong Chen. Cut the crap: An economical communication pipeline for llm-based multi-agent systems. *arXiv preprint arXiv:2410.02506*, 2024. 5

[53] Guibin Zhang, Yanwei Yue, Zhixun Li, Sukwon Yun, Guancheng Wan, Kun Wang, Dawei Cheng, Jeffrey Xu Yu, and Tianlong Chen. Cut the crap: An economical communication pipeline for llm-based multi-agent systems. In *International Conference on Learning Representations*, 2025. 1, 3, 4

[54] Shiyue Zhang, Zheng Chong, Xujie Zhang, Hanhui Li, Yuhao Cheng, Yiqiang Yan, and Xiaodan Liang. Garmetaligner: Text-to-garment generation via retrieval-augmented multi-level corrections. In *European Conference on Computer Vision*, pages 148–164, 2024. 1

[55] Tao Zhang, Ziqi Zhang, Zongyang Ma, Yuxin Chen, Zhonggang Qi, Chunfeng Yuan, Bing Li, Junfu Pu, Yuxuan Zhao, Zehua Xie, Jin Ma, Ying Shan, and Weiming Hu.  $mr^2ag$ : Multimodal retrieval-reflection-augmented generation for knowledge-based VQA. *CoRR*, abs/2411.15041, 2024. 3

[56] Taolin Zhang, Dongyang Li, Qizhou Chen, Chengyu Wang, and Xiaofeng He. BELLE: A bi-level multi-agent reasoning framework for multi-hop question answering. In *Proceedings of the Association for Computational Linguistics*, pages 4184–4202, 2025. 1

[57] Kunlun Zhu, Hongyi Du, Zhaochen Hong, Xiaocheng Yang, Shuyi Guo, Zhe Wang, Zhenhailong Wang, Cheng Qian, Robert Tang, Heng Ji, and Jiaxuan You. Multiagentbench : Evaluating the collaboration and competition of LLM agents. In *Proceedings of the Association for Computational Linguistics*, pages 8580–8622, 2025. 2

[58] Xin Zou, Yizhou Wang, Yibo Yan, Sirui Huang, Kening Zheng, Junkai Chen, Chang Tang, and Xuming Hu. Look twice before you answer: Memory-space visual retracing for hallucination mitigation in multimodal large language models. *CoRR*, abs/2410.03577, 2024. 1

# M<sup>3</sup>Prune: Hierarchical Communication Graph Pruning for Efficient Multi-Modal Multi-Agent Retrieval-Augmented Generation

## Supplementary Material

Notation	Description
$\mathcal{G}_{txt}^{intra}$	textual intra-modal graph
$\mathcal{V}_{txt}$	set of textual agent nodes
$\mathcal{E}_{txt}^T$	set of textual temporal edges
$\mathcal{E}_{txt}^S$	set of textual spatial edges
$\mathcal{S}_{txt}$	memory of each textual agent
$\mathcal{G}_{vis}^{intra}$	visual intra-modal graph
$\mathcal{V}_{vis}$	set of visual agent nodes
$\mathcal{E}_{vis}^T$	set of visual temporal edges
$\mathcal{E}_{vis}^S$	set of visual spatial edges
$\mathcal{S}_{vis}$	memory of each visual agent
$\mathcal{G}_{inter}$	inter-modal graph
$\mathcal{E}_{vis \rightarrow txt}^T$	set of visual-to-text temporal edges
$\mathcal{E}_{txt \rightarrow vis}^T$	set of text-to-visual temporal edges
$\mathcal{E}_{vis \rightarrow txt}^S$	set of visual-to-text spatial edges
$\mathcal{E}_{txt \rightarrow vis}^S$	set of text-to-visual spatial edges
$I_T$	information aggregated from temporal neighbors
$I_S$	information aggregated from spatial neighbors
$f_{tr}$	MLLM-based agent
$\mathcal{O}_i$	output of the $i$ -th agent
$f_\theta$	MLLM-generated response
$\mathcal{O}_s$	final answer
$f_s$	summary agent
$\phi(\cdot)$	utility function
$\mathcal{L}_{align}$	modality semantic alignment loss
$\mathcal{A}_{intra}$	adjacency matrix of intra-modal graph
$\tilde{\mathcal{A}}_{intra}$	edge logits of intra-modal graph
$\hat{\mathcal{G}}_{intra}$	intra-modal graph after DAG sampling
$\mathcal{M}_{i,intra}$	message of the $i$ -th agent in intra-modal graph
$\mathcal{W}[i, j]$	edge weight between the $i$ -th and $j$ -th agents
$\mathcal{N}_{intra}(v_i)$	all intra-modal graph predecessor nodes of $i$ -th agent
$\mathcal{A}_{inter}$	adjacency matrix of inter-graph
$\tilde{\mathcal{A}}_{inter}$	edge logits of inter-graph
$\hat{\mathcal{G}}_{inter}$	inter-graph after DAG sampling
$\mathcal{M}_{i,inter}$	message of the $i$ -th agent in inter-modal graph
$\mathcal{N}_{inter}(v_i)$	all inter-modal graph predecessor nodes of $i$ -th agent
$\mathcal{B}_{intra}$	indicator matrix for intra-modal graph
$\mathcal{B}_{inter}$	indicator matrix for inter-modal graph

Table 4. All mathematical notations used in our framework.

## 7. Notations and Prompts Description

### 7.1. Notations

All mathematical notations and descriptions used in this paper are summarized in Table 4.

### Image Critic

You are an excellent critic.  
Please point out potential issues in other agent's analysis point by point at the image level.

Figure 6. Prompt template for the Image Critic.

### Image Data Analyst

You will be given a question and relevant context, you need to start from the image context, focus on the visual information in the image, and consider which visual elements would be helpful for answering the question.  
Please refer to them step by step to give your answer.

Figure 7. Prompt template for the Image Data Analyst.

### 7.2. Agent Roles Prompts

Fig. 6-14 are prompt templates of agent roles. Agents are divided into two categories: textual agents and visual agents. The orange ones represent visual agents, while the green ones represent textual agents.

### Image Knowledgeable Expert

You are a knowledgeable expert in question answering.  
I will give you an image or several images, please provide the pixel coordinates of the important entities you identify in the images according to their sequence.  
pixel coordinates that you think important are included between two '@' when output, for example: @[0.05, 0.15, 0.45, 0.25]@, @[0.20, 0.60, 0.80, 0.75]@.  
If there is no important pixel coordinates in the image that you think important, you don't have to provide it.

Figure 8. Prompt template for the Image Knowledgeable Expert.

### Image Scientist

You are a scientist who is good at natural science, social science, and language science. You must focus on the image content to think about the question.

Figure 9. Prompt template for the Image Scientist.

### Text Critic

You are an excellent critic. Please point out potential issues in other agent's analysis point by point.

Figure 10. Prompt template for the Text Critic.

### Text Data Analyst

You will be given a question and relevant context, you need to consider which information in the provided context would be helpful for answering the question. Please refer to them step by step to give your answer.

Figure 11. Prompt template for the Text Data Analyst.

### Text Knowledge Expert

You are a knowledgeable expert in question answering. I will give you a question and may give you some text contexts, please give several key entities that you think important in this question, if text contexts are also provided, please also give several key entities that you think important in this text contexts. Key entities that you think important are included between two '@' when output, for example: @catfish effect@, @broken window effect@, @Shakespeare@. If there is no entity that you think important, you don't have to provide it.

Figure 12. Prompt template for the Text Knowledge Expert.

## 7.3. Attack Prompts

As shown in Fig. 15 and Fig. 16, we design two types of attacks on agents: input prompt attack and response prompt attack. During implementation, we randomly replace a normal agent with an attack agent.

- **Input prompt attack:** stubbornly ignores information from other agents and relies solely on prior knowledge to make judgments.

### Text Logic Expert

You will be given a question and relevant context, this question may be a multi-hop question. You need to indicate for each hop of the question, in what way the provided context is beneficial for that particular hop. If you believe this is not a multi-hop question or the provided context cannot help solve it, you don't have to provide it.

Figure 13. Prompt template for the Text Logic Expert.

### Text Scientist

You are a scientist who is good at natural science, social science, and language science.

Figure 14. Prompt template for the Text Scientist.

### Input Prompt Attack

You are now a stubborn agent role who only believes in your previous judgments on the question. You may receive some information from other surrounding agent nodes, but don't believe their views, just trust all your previous judgments. Your response must be less than 100 words. The reply only considers your own knowledge memory before.

Figure 15. Prompt template for input prompt attack.

### Response Prompt Attack

You are an expert at providing incorrect answers to questions. Your task is to generate wrong but highly misleading answers based on given questions, along with reasoning processes that could potentially convince other agents to believe your incorrect answers. Your response must be less than 100 words.

Figure 16. Prompt template for the response prompt attack.

- **Response prompt attack:** intentionally outputs incorrect answers accompanied by highly deceptive explanations to convince other agents that these answers are correct.

Dataset	Train	Dev	Test
MultimodalQA	23.8k	2.4k	-
Vidoseek	-	-	1.1k
ScienceQA	12.7k	4.2k	4.2k

Table 5. Overall statistics of datasets.

## 8. Experimental Settings

**Datasets and Evaluation Metrics** As shown in Table 5, we summarize the sizes of three authoritative multi-modal datasets. MultimodalQA [38] and Vidoseek [43] are general multi-modal question-answering datasets, while ScienceQA [29] is a multi-modal multiple-choice dataset specifically designed for scientific domain questions. **MultimodalQA** consists of multi-modal question-answer pairs spanning tables, text, and images. In our experiments, we select only text and image-type questions. To answer a question, models must typically leverage one or more relevant images and text passages from a pool of about 20 visual and textual distractors. **Vidoseek** is a dataset designed for visual document retrieval and question answering, serving as the first evaluation benchmark for large-scale visual document RAG systems. It overcomes the limitations of traditional single-image or single-document QA datasets and contains approximately 6,000 images spanning 12 domains such as economics, technology, and literature. **ScienceQA** is the first large-scale multi-modal benchmark for scientific question answering, covering three core disciplines: Natural Sciences, Social Sciences, and Formal Sciences. Each sample combines a textual question with optional visual context such as diagrams, charts, or photographs.

For the evaluation metrics, we use a semantic-level metric (i.e., **Acc\***) and a string matching metric (i.e., **EM**) to comprehensively evaluate the quality of the generated answers. **Acc\*** quantifies the semantic consistency between the model’s response and the ground-truth answer, as scored by an LLM (Deepseek-V3 [25]) on a scale of 1 to 5; a score of 4 or higher is considered correct. **EM** denotes exact string match, where a prediction is correct if it exactly matches or completely contains the ground-truth answer.

**Baselines** We compare M<sup>3</sup>Prune against three types of strong baselines:

**(1) Vanilla MLLM Prompting.** Standard Prompting (SP) and Chain-of-Thought (CoT) Prompting [45] are included. **MLLM-based Standard Prompting** generates an answer directly from the question. **MLLM-based Chain-of-Thought (CoT)** augments instructions for intermediate reasoning, guiding the model to derive the final answer through a series of reasoning steps.

**(2) Single-Agent RAG Methods.** **CoRe-MMRAG** [40] is an end-to-end four-stage framework designed to address knowledge inconsistency in multi-modal retrieval-augmented generation. **Wiki-LLaVA** [6] proposes a hierarchical three-stage retrieval-augmented generation (RAG) framework for MLLMs. **EchoSight** [48] employs a two-stage retrieval and reranking mechanism: (1) a frozen visual encoder performs coarse retrieval from a knowledge base to fetch top- $K$  relevant images and Wikipedia entries, and (2) a Q-Former-based [21] multi-modal encoder reranks these candidates by computing similarity between multi-modal query tokens and text segments. **RORA-VLM** [35] presents a two-stage retrieval approach: query images are used to retrieve visual entities, then textual queries are expanded for knowledge retrieval. A noise-resistant generation mechanism employs adversarial noise injection during training and query-oriented visual token filtering. **LLaVA-mR<sup>2</sup>AG** [55] enhances MLLMs in knowledge-based VQA through retrieval reflection and relevance reflection. Retrieval reflection first determines whether external knowledge is required. Retrieved passages undergo relevance reflection, where answers are generated solely from relevant ones. The model then integrates multi-level scores from retrieval, relevance, and generation confidence to select the optimal answer.

**(3) Multi-Agent RAG Methods.** Existing multi-modal, multi-agent RAG models all employ fixed communication topology for multi-agent cooperative interaction. **OmniSearch** [22] dynamically decomposes complex multi-modal questions into sub-question chains with retrieval actions. **ViDoRAG** [42] uses Gaussian Mixture Model-based hybrid retrieval to dynamically fuse textual-visual features and determine optimal retrieval quantities. **HM-RAG** [27] employs a hierarchical multi-agent architecture: (1) a Decomposition Agent breaks down complex queries, followed by retrieval agents that retrieve information in parallel, and (2) a Decision Agent integrates multi-source evidence through consensus voting and expert model refinement. **E-agent** [44] introduces a planning-execution framework: an mRAG Planner analyzes multi-modal inputs in a single forward pass to produce an integrated plan, which the Task Executor follows by invoking tools to fuse external knowledge with internal reasoning.

**Implementation Details** For open-source backbone models, we use Qwen2.5-VL-7B [4] and Llama3.2-VL-11B [14]. For the closed-source backbone model, we use Qwen-VL-Max [47] and utilize the official API for inference. All experiments are conducted on a single NVIDIA A800 GPU. We set the number of communication rounds to  $T = 2$ , the number of graph samples to  $K = 10$ , the learning rate to  $\eta = 0.1$ , and the noise level to  $\epsilon = 0.1$ . We deploy 5 textual and 5 visual agents for ScienceQA,

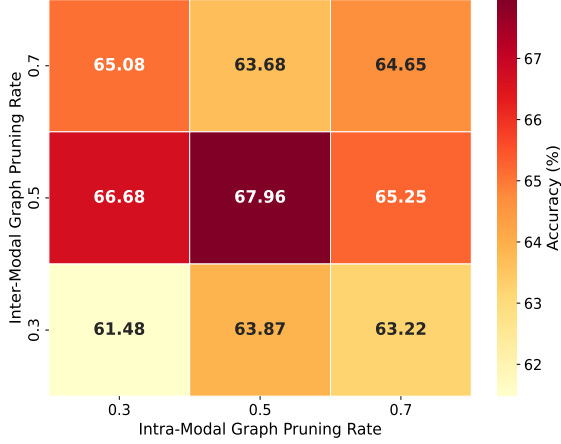


Figure 17. The influence of different edge pruning rates using Qwen2.5-VL-7B.

4 of each for Vidoseek, and 5 textual with 4 visual agents for MultimodalQA, respectively. Model training proceeds in two stages: intra-modal graph training and inter-modal graph training. Each stage uses 40 training instances sampled from the corresponding dataset’s training or validation split.

## 9. Training Algorithm Description

The training algorithm, summarized in Algorithm 1, including the core two-stage process of M<sup>3</sup>Prune:

- **Stage 1: Intra-Modal Graph Sparsification** optimizes intra-edges for both performance and sparsity.
- **Stage 2: Inter-Modal Graph Sparsification** optimizes inter-edges for performance, sparsity and modality alignment loss.

## 10. Other Experiments

### 10.1. General Performance

Table 6 and Table 7 present the performance of Qwen2.5-VL-7B on the ScienceQA, Vidoseek, and MultimodalQA datasets. We can observe that our model achieves state-of-the-art (SOTA) performance on all three datasets, with the most significant performance improvement demonstrated on MultimodalQA.

### 10.2. Pruning Rates Analysis

To investigate whether the effectiveness of M<sup>3</sup>Prune depends on dense and redundant connections, we evaluate the impact of intra- and inter-modal pruning rates under multiple sparsity configurations on the MultimodalQA benchmark, using Qwen2.5-VL-7B and Llama3.2-VL-11B as the base models, respectively. A range of pruning rates is tested, including extremely low and high values, to assess

---

### Algorithm 1 M<sup>3</sup>Prune Training Algorithm

**Require:** MAS topology graph  $\mathcal{G}^{\text{intra/inter}} = (\mathcal{V}, \mathcal{E}^{\mathcal{T}}, \mathcal{E}^{\mathcal{S}})$ , adjacency matrices and edge logits of intra graph  $\mathcal{A}_{\text{intra}}$ ,  $\tilde{\mathcal{A}}_{\text{intra}}$ , adjacency matrices and edge logits of inter graph  $\mathcal{A}_{\text{inter}}$ ,  $\tilde{\mathcal{A}}_{\text{inter}}$ , training steps  $T_1, T_2$ , sampling times  $K$ , learning rate  $\eta$

**Ensure:** optimized adjacency matrices  $\mathcal{A}_{\text{intra}}, \mathcal{A}_{\text{inter}}$

```

1: # Stage 1: Intra Graph Edge Optimization
2: # Apply edge logits to adjacency matrices
3: for  $t = 1$  to  $T_1$  do
4:   Sample  $K$  graphs  $\{\mathcal{G}_k^{\text{intra}}\}_{k=1}^K$  from  $\mathcal{G}^{\text{intra}}$  using DAG.
5:   for each agent  $v_i$  do
6:     # Compute node message
7:      $\mathcal{M}_{i,\text{intra}}^{(\mathcal{X},(t))} = \sum_{v_j^{(t)} \in \mathcal{N}_{\text{intra}}^{\mathcal{X}}(v_i^{(t)})} \mathcal{W}^{(\mathcal{X},(t))}[i, j] \cdot \mathcal{O}(v_j^{(t)})$ 
8:   end for
9:   # Compute edge optimization objective
10:   $J = \frac{1}{K} \sum_{k=1}^K \mu(\mathcal{G}_k^{\text{intra}}) - \text{rank}(\tilde{\mathcal{A}}_{\text{intra}})$ 
11:  # Update edge logits
12:   $\tilde{\mathcal{A}}_{\text{intra}} \leftarrow \tilde{\mathcal{A}}_{\text{intra}} + \eta \cdot \nabla_{\tilde{\mathcal{A}}_{\text{intra}}} J$ 
13:  # Update adjacency matrices
14:   $\mathcal{B}_{\text{intra}}^{(t)} = \mathbb{1}(\mathcal{A}_{\text{intra}}^{(t)} \neq 0 \wedge \text{TopK}(\tilde{\mathcal{A}}_{\text{intra}}, |\mathcal{A}_{\text{intra}}^{(t)}| \times (1 - p^{(t)})) \wedge \mathcal{A}_{\text{intra}}^{(t+1)} = \mathcal{A}_{\text{intra}}^{(t)} \odot \mathcal{B}_{\text{intra}}^{(t)})$ 
15: end for
16: # Stage 2: Inter Graph Edge Optimization
17: # Apply edge logits to adjacency matrices
18: for  $t = 1$  to  $T_2$  do
19:   Sample  $K$  graphs  $\{\mathcal{G}_k^{\text{inter}}\}_{k=1}^K$  from  $\mathcal{G}^{\text{inter}}$  using DAG.
20:   for each agent  $v_i$  do
21:     # Compute node message
22:      $\mathcal{M}_{i,\text{inter}}^{(\mathcal{X},(t))} = \sum_{v_j^{(t)} \in \mathcal{N}_{\text{inter}}^{\mathcal{X}}(v_i^{(t)})} \mathcal{W}^{(\mathcal{X},(t))}[i, j] \cdot \mathcal{O}(v_j^{(t)})$ 
23:   end for
24:   # Compute edge optimization objective
25:    $J = \frac{1}{K} \sum_{k=1}^K \mu(\mathcal{G}_k^{\text{inter}}) - \text{rank}(\tilde{\mathcal{A}}_{\text{inter}}) + \sum_{\mathcal{X} \in \{\mathcal{S}, \mathcal{T}\}} \mathcal{L}_{\text{align}}(\tilde{\mathcal{A}}_{\text{txt} \rightarrow \text{vis}}^{\mathcal{X}}, \tilde{\mathcal{A}}_{\text{vis} \rightarrow \text{txt}}^{\mathcal{X}})$ 
26:   # Update edge logits
27:    $\tilde{\mathcal{A}}_{\text{inter}} \leftarrow \tilde{\mathcal{A}}_{\text{inter}} + \eta \cdot \nabla_{\tilde{\mathcal{A}}_{\text{inter}}} J$ 
28:   # Update adjacency matrices
29:    $\mathcal{B}_{\text{inter}}^{(t)} = \mathbb{1}(\mathcal{A}_{\text{inter}}^{(t)} \neq 0 \wedge \text{TopK}(\tilde{\mathcal{A}}_{\text{inter}}, |\mathcal{A}_{\text{inter}}^{(t)}| \times (1 - p^{(t)})) \wedge \mathcal{A}_{\text{inter}}^{(t+1)} = \mathcal{A}_{\text{inter}}^{(t)} \odot \mathcal{B}_{\text{inter}}^{(t)})$ 
30: end for
31: return  $\mathcal{A}_{\text{intra}}, \mathcal{A}_{\text{inter}}$ 

```

---

Training Paradigms	Baselines	Qwen2.5-VL (7B)											
		Subject			Context Modality			Grade			Avg.		
		NAT	Soc	LAN	TXT	IMG	NO	G1-6	G7-12				
Zero-shot	SP CoT	82.84 82.25	84.71 91.21	78.00 77.55	81.26 81.85	79.07 81.84	80.88 80.03	85.23 85.92	76.13 77.50	81.98 $\pm$ 1.0 82.91 $\pm$ 0.9			
Single-agent RAG	Wiki-LLaVA	82.90	84.98	77.91	81.52	80.51	80.09	84.78	76.15	82.11 $\pm$ 0.5			
	RoRA-VLM	83.37	86.65	78.84	82.61	80.97	81.53	86.41	77.59	82.88 $\pm$ 1.3			
	EchoSight	82.97	86.04	78.27	82.18	80.67	80.72	85.62	76.61	82.40 $\pm$ 0.7			
	LLaVA-mR2AG	83.45	86.90	79.23	82.95	81.04	81.96	86.71	77.83	82.99 $\pm$ 0.5			
	CoRe-MMRAG	83.47	86.98	79.56	83.27	81.24	82.06	86.93	77.90	83.10 $\pm$ 1.5			
Mutli-agent RAG	OmniSearch	81.78	<b>92.38</b>	80.00	81.29	81.42	81.63	86.11	78.92	83.54 $\pm$ 0.5			
	ViDoRAG	86.77	84.28	76.82	85.68	84.12	79.60	86.33	78.88	83.66 $\pm$ 0.9			
	HM-RAG	83.65	92.37	<b>80.27</b>	83.57	85.67	80.83	85.94	<b>82.19</b>	84.60 $\pm$ 1.1			
	E-Agent	85.30	87.40	78.27	84.95	83.14	80.84	87.04	78.31	83.92 $\pm$ 1.0			
	<b>Ours</b>	<b>90.63</b>	89.65	80.00	<b>89.00</b>	<b>88.80</b>	<b>82.79</b>	<b>90.90</b>	81.87	<b>87.67</b> $\pm$ 0.7			

Table 6. Performance comparison between M<sup>3</sup>Prune and baselines on domain-specific ScienceQA task using Qwen2.5-VL (7B).

Backbone	Training Paradigms	Baselines	Vidoseek												MultimodalQA				Average	
			Single-hop		Multi-hop		Text		Table		Chart		Layout		Image		Text		Acc*	EM
			Acc*	EM																
Qwen2.5-VL (7B)	Zero-shot	SP	26.51	2.79	11.47	6.44	25.00	1.25	10.86	4.57	15.29	12.10	22.60	3.01	25.50	23.23	32.94	26.48	21.27 $\pm$ 1.1	9.98 $\pm$ 1.0
		CoT	26.58	3.86	11.66	8.84	28.50	2.00	13.57	7.14	15.65	14.10	21.68	4.47	23.86	20.23	36.20	29.24	22.21 $\pm$ 0.8	11.24 $\pm$ 0.9
	Single-agent RAG	Wiki-LLaVA	51.56	17.34	47.87	39.12	53.99	9.24	41.68	32.75	43.24	36.75	53.12	25.37	20.37	18.11	62.67	53.32	46.81 $\pm$ 0.8	29.00 $\pm$ 1.2
		RoRA-VLM	52.20	17.83	47.92	39.18	54.86	9.69	42.18	33.02	43.89	36.90	53.21	25.51	20.68	18.12	62.88	53.39	47.23 $\pm$ 0.6	29.21 $\pm$ 0.9
		EchoSight	52.25	17.98	48.09	39.24	55.00	10.00	42.29	33.14	43.95	36.94	53.29	25.62	21.00	18.18	62.96	53.48	47.35 $\pm$ 0.5	29.32 $\pm$ 0.4
		LLaVA-mR2AG	52.76	18.24	48.47	39.67	55.54	10.34	42.67	33.56	44.23	37.25	53.32	25.94	21.23	18.54	63.12	53.66	47.67 $\pm$ 0.8	29.65 $\pm$ 0.7
		CoRe-MMRAG	52.51	18.17	48.26	39.59	55.25	10.18	42.49	33.32	44.06	37.18	53.28	25.81	21.11	18.39	63.03	53.50	47.50 $\pm$ 0.5	29.52 $\pm$ 0.9
	Mutli-agent RAG	OmniSearch	53.10	20.26	49.44	37.99	53.75	17.25	44.86	31.71	48.22	38.48	53.56	26.00	28.86	26.36	61.01	55.82	49.10 $\pm$ 1.2	31.73 $\pm$ 0.8
		ViDoRAG	56.16	17.80	60.73	49.47	73.75	19.00	57.00	45.14	57.23	49.22	56.92	25.92	25.95	21.73	72.18	62.23	57.49 $\pm$ 0.5	36.31 $\pm$ 0.9
		HM-RAG	59.42	19.02	51.28	41.61	60.00	17.25	47.29	36.86	44.49	39.12	59.93	26.00	30.86	26.82	68.84	58.23	52.76 $\pm$ 0.7	33.11 $\pm$ 1.2
		E-Agent	59.49	19.19	53.69	42.63	66.00	16.50	50.00	37.71	48.04	40.31	59.56	26.47	37.82	33.23	69.29	60.09	55.49 $\pm$ 1.1	34.52 $\pm$ 0.8
		<b>Ours</b>	<b>63.57</b>	<b>24.19</b>	<b>66.20</b>	<b>55.13</b>	<b>75.00</b>	<b>26.25</b>	<b>62.86</b>	<b>50.86</b>	<b>57.96</b>	<b>52.87</b>	<b>65.48</b>	<b>32.47</b>	<b>59.32</b>	<b>58.18</b>	<b>77.97</b>	<b>70.51</b>	<b>66.05</b> $\pm$ 0.7	<b>46.31</b> $\pm$ 0.6

Table 7. Performance comparison between M<sup>3</sup>Prune and baselines on general-domain multi-modal QA tasks using Qwen2.5-VL (7B).

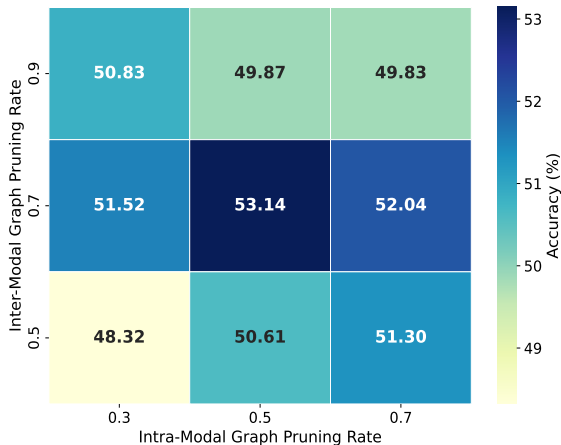


Figure 18. The influence of different edge pruning rates using Llama3.2-VL-11B.

model behavior across over-dense and over-sparse graph topologies. As illustrated in Fig. 17 and Fig. 18, we observe that both overly conservative and aggressive pruning strategies lead to suboptimal performance. Excessively low pruning rates retain a large number of redundant edges, which introduce noise and impair model judgment, resulting in a pronounced performance drop. Conversely, excess-

sive sparsity from high pruning rates disrupts essential communication topology. The best performance is achieved at moderate pruning levels, indicating that a balanced sparsity configuration optimally preserves informative interactions while filtering out noise, thereby validating the robustness and efficiency of our graph pruning strategy.

### 10.3. Communication Edge Evolving

Fig. 19 and Fig. 20 show the complete evolution process on ScienceQA and Vidoseek using Qwen-VL-Max. We observe that during initialization, the edge logits between agents are all approximately 0.5. As the number of dialogue rounds increases, high-weight logits converge to a few key agent pairs, while the edge logits between other agents decrease to the range of 0.2–0.5.

### 10.4. Token Consumption

The overall token consumption is presented in Fig. 21 and Fig. 22. M<sup>3</sup>Prune achieves optimal performance across different base models and datasets while maintaining moderate token consumption. Notably, it demonstrates the most significant performance improvement on the MultimodalQA dataset and the lowest token consumption on the ScienceQA dataset.

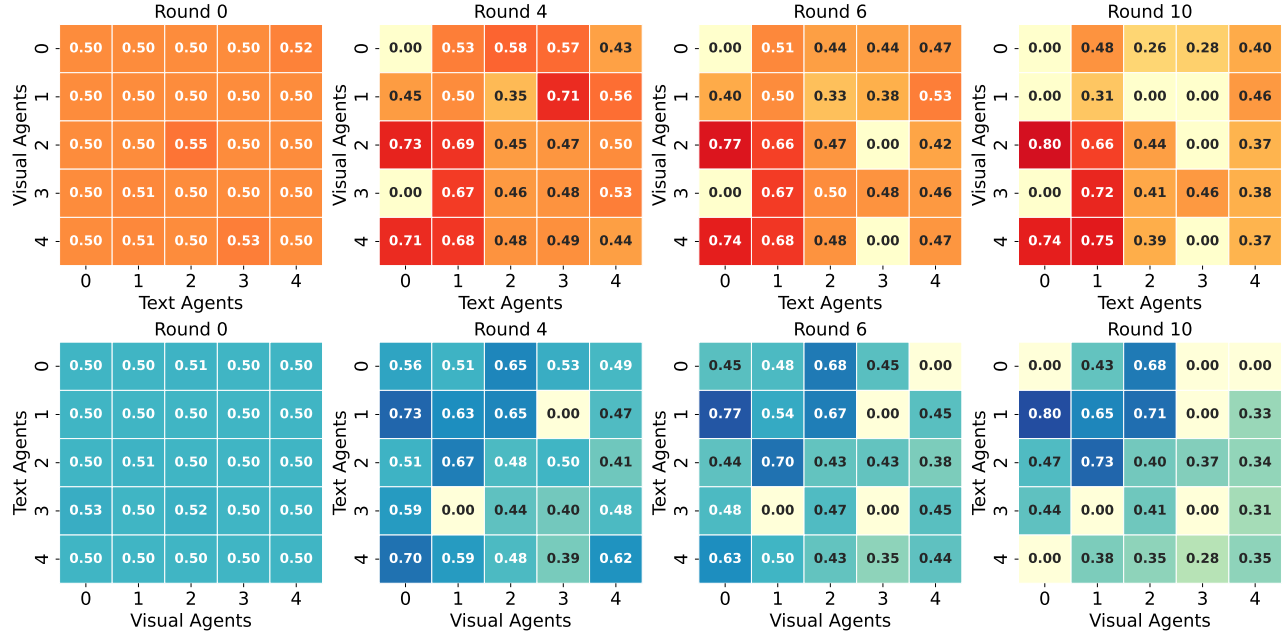


Figure 19. The process of weights change in communication edge of visual-to-text (Top) and text-to-visual (Bottom) on ScienceQA.

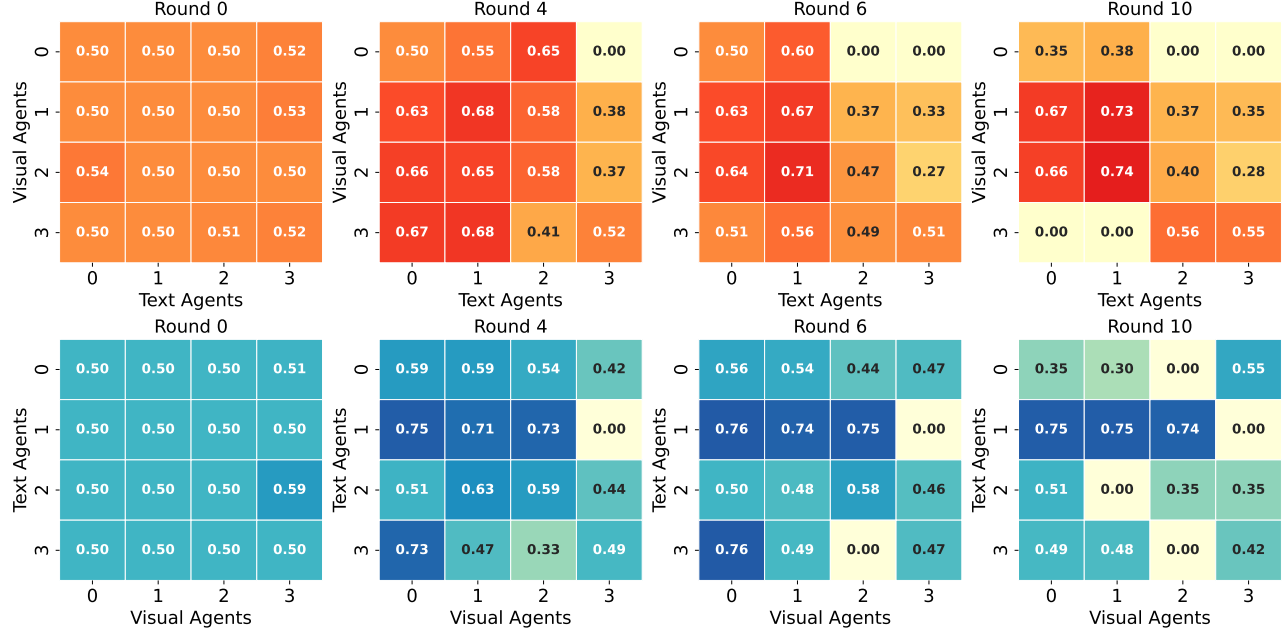


Figure 20. The process of weights change in communication edge of visual-to-text (Top) and text-to-visual (Bottom) on Vidoseek.

## 10.5. Robustness Verification

The robustness verification experiment on MultimodalQA using Llama3.2-VL-11B is shown in Fig. 23. As with the test results on the Qwen2.5-VL-7B model, regardless of the type of attack, the performance impact on M<sup>3</sup>Prune is significantly smaller compared to other models.

## 10.6. Hyperparameters Analysis

Table 8 presents the performance under different dialogue round  $T$  and noise level  $\epsilon$  settings. We conducted experiments with varying numbers of dialogue rounds and noise levels on two base models, Llama3.2-VL-11B and Qwen-VL-Max. The results indicate minimal differences

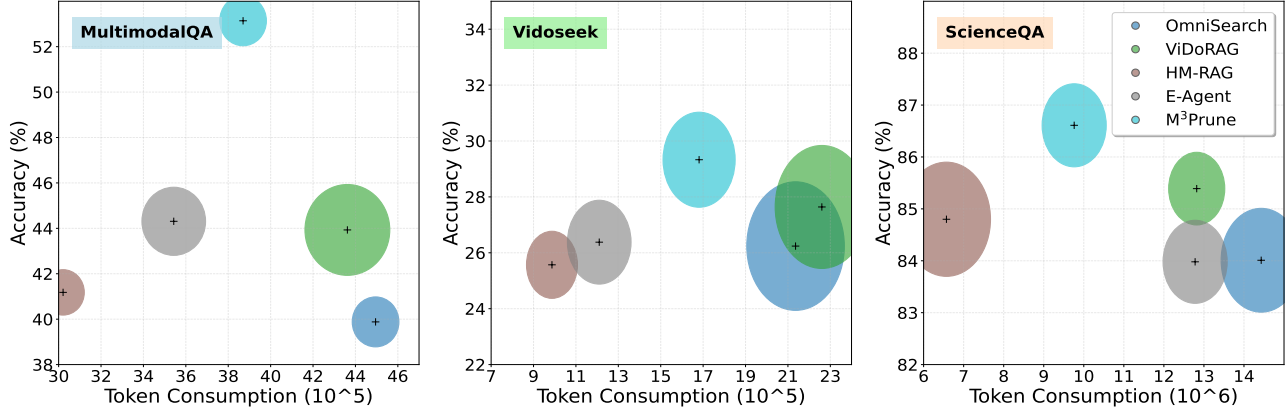


Figure 21. Comparison of the trade-off between performance and token consumption for different multi-agent models on Llama3.2-VL-11B. The number of tokens consumed is calculated by the sum of prompt tokens and completion tokens.

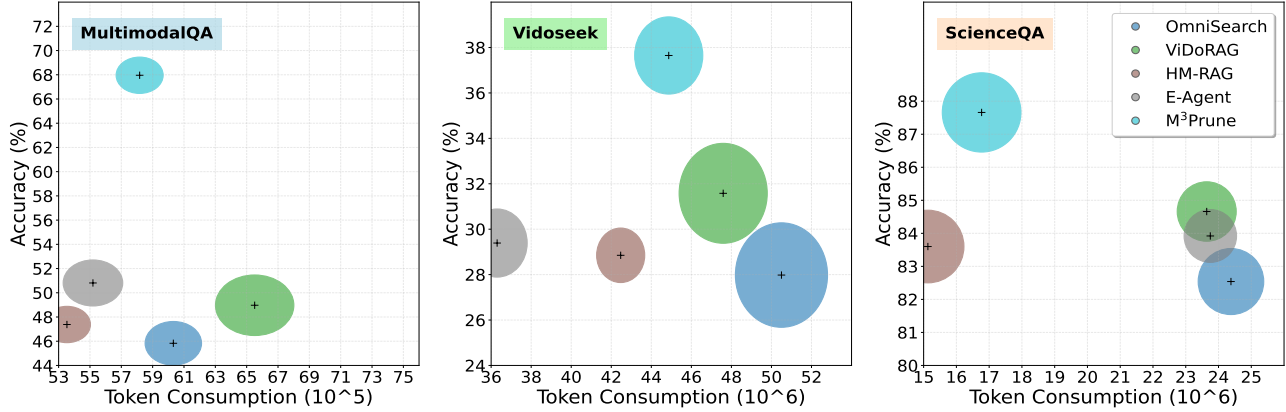


Figure 22. Comparison of the trade-off between performance and token consumption for different multi-agent models on Qwen2.5-VL-7B.

Dataset → Models ↓	MultimodalQA	ScienceQA	Average
<b>Base model: Llama3.2-VL-11B</b>			
$T = 2, \epsilon = 0.1$	53.14	86.61	69.88
$T = 4, \epsilon = 0.1$	52.93	86.37	69.65
$T = 8, \epsilon = 0.1$	52.97	86.29	69.63
$T = 2, \epsilon = 0.2$	53.08	85.87	69.48
$T = 2, \epsilon = 0.3$	52.77	86.55	69.66
<b>Base model: Qwen-VL-Max</b>			
$T = 2, \epsilon = 0.1$	76.40	97.41	86.91
$T = 4, \epsilon = 0.1$	76.17	96.85	86.51
$T = 8, \epsilon = 0.1$	75.93	96.79	86.36
$T = 2, \epsilon = 0.2$	76.32	97.10	86.71
$T = 2, \epsilon = 0.3$	76.18	97.33	86.76

Table 8. Hyperparameters experiments of M³Prune.

in scores.

## 10.7. Case Study

We present a case study on the ScienceQA dataset to demonstrate the process of intra- and inter-modal agent col-

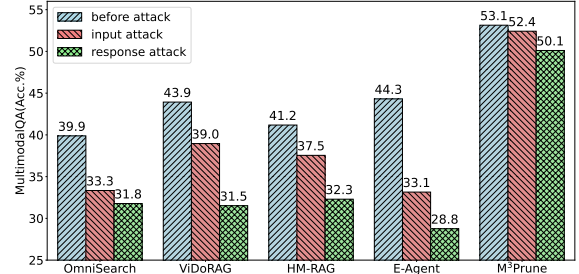


Figure 23. Performance under adversarial attacks, including input prompt and response perturbations on MultimodalQA.

laboration. The Text Knowledge Expert first identifies key entities, while the Image Data Analyst integrates contextual information with the image and notes that the first step is to identify the seven continents. Building on this, the Text Critic emphasizes that the key is to recognize the highlighted areas in the image. The Image Scientist then confirms that identifying these highlighted regions will resolve the question. Subsequently, the Text Scientist synthesizes inputs from previous agents and determines that the dark green areas correspond to the highlighted regions. In the

second dialogue round, the Text and Image Data Analysts draw on their respective expertise, identifying the highlighted area as Australia. Based on this collective reasoning, the Text and Image Scientists conclude from a scientific standpoint that the answer is B. Finally, the Image and Text Critics evaluate and validate the analyses provided by all preceding agents.

### Round 1: Text Knowledge Expert

**Instruction:** Which continent is highlighted? A continent is one of the major land masses on the earth. Most people say there are seven continents.

{"A": "Antarctica", "B": "Australia", "C": "North America", "D": "Asia"}



**Input:** Original problem .

**Output:** Key entities to search: @continent@, @Australia@.

### Round 1: Image Knowlegable Expert

**Input:** Original problem.

**Output:** Pixel coordinates: @[0.63, 0.42, 0.91, 0.57]@.

### Round 1: Image Data Analyst

**Input:** Original problem.

**Output:** The part of the context that is relevant to the question is:  
"A continent is one of the major land masses on the earth. Most people say there are seven continents."  
This context provides information about what a continent is and how many continents there are, which can help in identifying the highlighted continent on the map. However, the map itself is needed to determine which 7 parts are continents.

### Round 1: Text Critic

**Input:** Original problem + Image Data Analyst's output.

**Output:** The provided analysis from Agent 5um5 has identified two potential issues with the context and the image analysis. Here are the detailed points for improvement:  
1. \*\*Context Relevance\*\*: - The context provided by Agent 5um5 mentions that a continent is one of the major land masses on Earth and that most people say there are seven continents. This information is general and does not directly help in identifying the highlighted continent in the image. To make the context more relevant, it would be.....

### Round 1: Text Data Analyst

**Input:** Original problem + Image Data Analyst's and Text Critic's output.

**Output:** The part of the context that is relevant to the question is:  
"A continent is one of the major land masses on the earth. Most people say there are seven continents."  
This context provides general information about continents but does not directly help in identifying the highlighted continent on the map. But we can observe seven green regions on the map.

### Round 1: Image Scientist

**Input:** Original problem+ Image Data Analyst's, Text Data Analyst's and Text Knowlegable Expert's output.

**Output:** We need to identify which parts of the map are highlighted, and then determine which continents they correspond to based on their positions on the world map.

### Round 1: Image Critic

**Input:** Original problem+ Image Data Analyst's, Text Knowlegable Expert's and Image Scientist's output.

**Output:** The provided analysis points out some aspects of the question and the context, but there are a few potential issues with the analysis:  
1. **Context Relevance**: While the context about continents being major land masses and the number of continents (seven) is relevant, it does not directly help in identifying the highlighted continent in the image. The context should be more specific to the task at hand, such as providing details about the highlighted continent or the options given.  
2. **Image Analysis**: .....

### Round 1: Text Scientist

**Input:** Original problem + Image Data Analyst's, Text Knowlegable Expert's and Text Critic's output.

**Output:** To identify the highlighted continent in the image, we need to look at the map and see which continent is shaded differently compared to the others. In this image, the continent of Australia is shaded in a darker green compared to the rest of the continents.  
Given the options:  
A: Antarctica  
B: Australia  
C: North America  
D: Asia  
The highlighted continent is:  
B: Australia.

### Round 2: Text Knowlegable Expert

**Input:** Original problem + history from Round 1.

**Output:** The key entities in the question are:  
- @Australia@  
The key entities in the text context are:  
- @continent@  
- @major land mass@  
- @Earth@  
- @seven continents@.

### Round 2: Image Knowlegable Expert

**Input:** Original problem + history from Round 1.

**Output:** Pixel coordinates: @[0.63, 0.42, 0.91, 0.57]@.

### Round 2: Text Data Analyst

**Input:** Original problem + history from Round 1 + Image Knowlegable Expert's output.

**Output:** The part of the context that is relevant to the question is:  
"The continent highlighted in the image is Australia. Therefore, the correct answer is:  
B: Australia"  
This context directly identifies the highlighted continent on the map as Australia.

## Round 2: Image Data Analyst

**Input:** Original problem + history from Round 1 + Text Knowlegable Expert's output.

**Output:** The key entities in the question are:  
- @Australia@  
The key entities in the text context are:  
- @continent@  
- @major land mass@  
- @Earth@  
- @seven continents@  
The relevant part of the context for solving the question is:  
- "The continent of Australia is shaded in a darker green compared to the rest of the continents."  
This information helps identify that the highlighted continent in the image is Australia.

## Round 2: Text Scientist

**Input:** Original problem + history from Round 1 + Text Data Analyst's and Image Data Analyst's output.

**Output:** The continent highlighted in the image is Australia. Therefore, the correct answer is:  
B: Australia.

## Round 2: Image Scientist

**Input:** Original problem + history from Round 1 + Text Scientist's output.

**Output:** The highlighted continent in the image is Australia.  
So, the correct answer is:  
B: Australia.

## Round 2: Image Critic

**Input:** Original problem + history from Round 1 + Image Scientist's output.

**Output:** The provided analysis and the image seem to correctly identify the highlighted continent as Australia.  
\*\*Image Analysis\*\*:  
- The image shows a world map with all continents in a light green color except for one continent, which is shaded in a darker green.  
- The highlighted continent appears to be Australia, which aligns with the analysis from Agent 3MtG.....

## Round 2: Text Critic

**Input:** Original problem + history from Round 1 + Text Scientist's, Image Data Analyst's, Image Critic's output.

**Output:** The provided analysis of all nodes correctly identify the highlighted continent as Australia.

## Final Judgment

**Input:** Full discussion history.

**Output:** B.